MECHANISMS OF MELANOMA CELL SURVIVAL AND MAINTENANCE: TARGETING APOPTOSIS AND AUTHOPHAGY TO IMPROVE DISEASE TREATMENT

by

Keith Garret Wolter

A dissertation submitted in partial fulfillment
of the requirements for the degree of
Doctor of Philosophy
(Cellular and Molecular Biology)
in The University of Michigan
2011

Doctoral Committee:

María S. Soengas, Co-Chair
Professor Thomas E. Carey, Co-Chair
Professor Gabriel Nunez
Associate Professor Colin S. Duckett

To my father,
James Garret Wolter,
who lost his fight with cancer during my time in the laboratory,
but never lost his spirit, his determination, or his unshakable faith in me.

Dad, you motivate me.

To my wife,
Jill Marie Mhyre,
who had to work twice as hard to support our family during my time in the laboratory, but never stopped supporting and loving me.

Jill, you sustain me.

To my daughter,
Fiona Skye Wolter,
who saw much less of me during my time in the laboratory than either of us would have liked, but who has brought me more joy than she will ever know.

Fi, you inspire me.

ACKNOWLEDGEMENTS

To all who helped me along the way, my sincere thanks. In particular, I'd like to thank Drs. Bradford, Carey and Soengas, for their guidance and instruction; Monique, Lionel, Chad and Josh, for their friendship and help; and finally Jill, for her patience and support.

TABLE OF CONTENTS

CHAPTER III

CHAPTER IV

CHAPTER V

LIST OF FIGURES

ABSTRACT

MECHANISMS OF MELANOMA CELL SURVIVAL AND MAINTENANCE: TARGETING APOPTOSIS AND AUTHOPHAGY TO IMPROVE DISEASE TREATMENT

by

Keith Garret Wolter

Co-chairs: María S. Soengas and Thomas E. Carey

Metastatic melanoma has proven exceptionally difficult to treat, in part due to consistent defects in cell death pathways. Overexpression of anti-apoptosis proteins from the Bcl-2 family is a hallmark of melanoma progression. Past strategies targeting these proteins have assumed equivalence between Bcl-2, Bcl-x_L and Mcl-1, closely related anti-apoptotic factors. Recent evidence, however, has shown that Bcl-2 family members display different binding affinities and survival activities. To assess the specific functions of Bcl-2, Bcl-x_L and Mcl-1 in melanoma cell survival, we used a genetic approach based on targeted RNA interference. We found that Mcl-1 is the key determinant of melanoma resistance to multiple chemotherapeutic agents. Importantly, Mcl-1 is dispensable for normal melanocyte viability, offering a window for therapeutic intervention. We sought to utilize these findings to overcome the resistance of

melanoma cells to proteasome inhibition. Proteasome inhibitors have shown great promise in treating certain cancers, but are ineffective as single agents against melanoma. Selective drug inhibition of Mcl-1, in combination with proteasome blockade, lead to the effective killing of melanoma cells, both *in vitro* and *in vivo*. Our studies suggest a functional hierarchy of Bcl-2 anti-apoptosis proteins that could be exploited to overcome melanoma resistance to proteasome inhibition.

More broadly, we sought to identify new mechanisms of melanoma chemoresistance. Electron microscopy of melanoma cells revealed the presence of autophagosomes in cells surviving after treatment with various chemotherapeutic agents. Multillamelar structures surrounding cellular organelles were particularly evident upon treatment with cyclopamine, an established inhibitor of Sonic Hedgehog signaling. These results were unexpected, as the Sonic Hedgehog pathway has not previously been linked to autophagy. The aberrant structures were sustained for extended periods, during which cells lacked proliferative capacity but remained viable. Notably, although early steps of autophagy were present in cyclopamine-treated cells, the later stage of autophagosome-lysosome fusion was absent. We hypothesized this autophagy blockade might provide a therapeutic opportunity. Indeed, forcing autophagy with hypoxia or low serum in the setting of cyclopamine treatment induced efficient melanoma cell killing. A better understanding of autophagy, a previously unexplored pathway in melanoma, may reveal new targets for therapy.

CHAPTER I

INTRODUCTION

The Scope of the Problem

The diagnosis of melanoma is one that fills both patient and physician with dread. While the surgical resection of a melanoma caught in its earliest stages can be curative, melanomas all too often have invaded the deeper layers of the skin and spread to lymph nodes and other distant sites prior to disease detection. In these cases, the prognosis is invariably quite poor: 5-year survival rates remain less than 5%, even with the best treatments currently available (1). Furthermore, the incidence of this disease continues to climb, rising ~5% per year in industrialized countries over the past 40 years (2). Melanoma incidence rates have increased in virtually all age and race groups (3). In the United States alone, >50,000 cases of melanoma are detected each year; despite accounting for only ~4% of skin cancers detected in the US, melanoma is responsible for ~75% of skin cancer deaths (4). Perhaps most sobering is the fact that FDA-approved chemotherapeutic regimens for the treatment of metastatic melanoma (both single agent and combination therapies) show no significant impact on patient survival, despite 30 years of research and clinical use (1).

Apoptosis and Melanoma Chemoresistance

While cancer cells are by nature resistant to many of the stressors that can cause the death of normal cells, melanoma cells are particularly resistant to cell-

death inducing agents (5). A diverse range of chemotherapeutic agents have been used to treat melanomas, but despite a variety of different cytotoxic mechanisms (i.e. DNA methylation (dacarbazine), DNA cross-linking (cisplatin), microtubule damage (vinblastine), et cetera), complete responses are observed in only 3 to 15% of patients, even when multiple agents are combined (4). Indeed, most tumor response is often only temporary; while sensitive tumor cells may undergo cell death, any effect is quickly outweighed by expansion of the remaining chemoresistant cells. Drug efflux, detoxification, and/or enhanced DNA repair all may play a role in treatment failures of current anti-melanoma agents. However, a number of studies have concluded that these mechanisms are not a general feature of aggressive melanomas. Instead, advanced melanomas present with a pleiotropic disregulation of apoptosis (6-10). The disruption of cell death pathways in malignant cells, a feature that has been termed a 'hallmark of cancer' (4), is thus a key underlying reason for melanoma treatment resistance.

The past 10 years have witnessed a prolific expansion in our understanding of the mechanisms underlying programmed cell death, and of how these mechanisms are altered in cancer. The tumor suppressor p53 plays a primary role in inducing cell death in response to many stressors, via both transcriptional -dependent and –independent pathways (11, 12). Intriguingly, however, p53 is rarely mutated or deleted in melanoma (13). (Figure 1.1) The molecular mechanisms underlying this paradox can be explained, at least in part, by alterations elsewhere in the cell death machinery in melanoma cells.

Changes in Apoptotic Cascades

Cell survival regulator proteins, located both upstream and downstream of p53, are some of the most common molecular deviations found in melanomas. For example, the p53 inhibitor HDM2 is frequently up-regulated in melanoma; reducing HDM2 levels sensitizes melanoma cells to apoptosis (14). Downstream from the mitochondria, the loss of apoptosis protease-activating factor (Apaf-1) has been noted in some melanomas, and correlates with resistance to chemotherapy (15, 16). Likewise, levels of death-inhibiting proteins downstream from the mitochondria in the apoptosis pathway, such as the IAPs (inhibitor of apoptosis proteins) and FLIPs (FLICE inhibitory proteins) are increased in melanoma. Specifically, higher expression levels of X-IAP, survivin, and ML-IAP (three different IAPs) are associated with tumor progression and poorer melanoma response to treatment (17-19); similar results have been demonstrated for cFLIP (20); see Figure 1.1. Recent work, utilizing both melanoma cells *in vitro* and melanoma xenograft models, has generated some promising preliminary results using agents which target the either the IAPs or cFLIP (19, 21, 22). Still, it is unclear whether and to what extent these alterations in apoptotic pathways have a causative role in melanoma development, versus simply representing by-products of tumor progression.

Figure 1.1

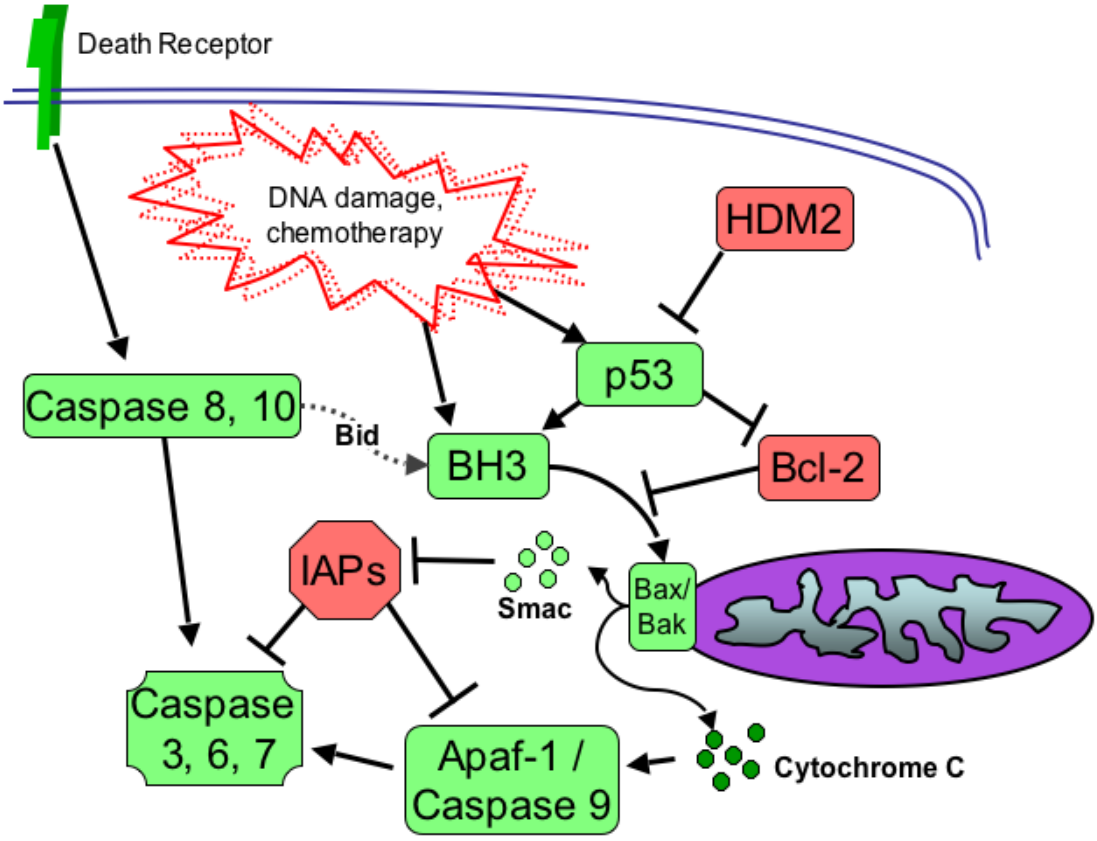

Figure 1.1 Simplified schematic of the pathways of apoptosis in mammalian cells. Pro-death molecules are shown in green. On the left, the extrinsic apoptotic pathway, activated via death receptor signal transduction, is propagated through initiator caspases 8 and 10, which in turn catalyze and activate the effector caspases 3, 6 and 7. On the right is the intrinsic or mitochondrial apoptotic pathway, which is controlled upstream by p53 and other sensors of DNA damage and cellular injury. Activation of Bax/Bak by BH3 only proteins leads to release of mitochondrial factors, including SMAC and Cytochrome *c*, into the cytosol. These factors trigger apoptosome formation by Apaf-1 and caspase 9. The apoptosome in turn activates the common effector caspases. At various points, the apoptosis inhibitors shown in red can act as antagonists or brakes on the cell death cascade.

The Bcl-2 Protein Family: A Hierarchy of Cell Death Control

Active investigations within the fields of melanoma and apoptosis have been focused on the Bcl-2 protein family, because several anti-apoptotic members (Bcl-2, Bcl-x_L and Mcl-1) are upregulated in advanced melanoma tumors (23). A main objective of this thesis was to define the relative contribution of Bcl-2, Bcl-x_L and Mcl-1 to melanoma maintenance and drug resistance. The stability and regulation of these proteins in melanoma was previously poorly known. In this chapter I will summarize aspects of the Bcl-2 family in the context of melanoma treatment. Subsequently, I will present a rationale for studying the contribution of the proteasome to the half-life of Bcl-2 family members, and ultimately, discuss our approach to dissect the specific role of Bcl-2 proteins to the response of melanoma cells to proteasome inhibitors.

Bcl-2 family members act as critical regulators of the intrinsic, or mitochondrial, arm of the apoptotic cascade (24-27). Bcl-2 proteins share an evolutionary heritage that can be traced back to the CED-9 and EGL-1 genes in *Caenorhabditis elegans*, but have developed increased complexity in higher eukaryotes. In mammals, Bcl-2 family members are categorized into three sub-groups: 1) pro-survival proteins, which include Bcl-2, Bcl-x_L, Mcl-1, A1, and Bcl-w; 2) pro-death effectors, such as Bax, Bak, and Bok; and 3) pro-death activators, or 'BH3-only' proteins, which is the largest and most structurally diverse sub-group and includes Bid, Bad, Bim, Bik, Hrk, Noxa, and PUMA (25, 28). As shown in Figure 1.2, all Bcl-2 family members contain a BH3 (Bcl-2 homology 3) domain, and most have a trans-membrane domain at their carboxyl

terminus; the pro-survival proteins and pro-death effectors also can have additional domains in common: BH1, BH2, and (in the pro-survival proteins) BH4.

The interplay between pro- and anti-apoptotic Bcl-2 family members is complex. In global terms, BH3-only activators initiate the formation of multimeric complexes of pro-death effectors on the outer membrane of the mitochondria (29, 30). The pro-survival Bcl-2 proteins, meanwhile, counter the formation of the pro-death complexes by inhibiting the BH3-only activity [reviewed recently in (28)]. The formation of Bax/Bak oligomers on mitochondria leads to mitochondrial outer membrane permeabilization (MOMP), and subsequently to the release of mitochondrial proteins, including cytochrome *c*, Smac, and Omi. These factors, once in the cytosol, initiate apoptosome formation and caspase activation, ultimately resulting in the hallmark changes of apoptosis. Recently, a more detailed understanding of the hierarchy within the Bcl-2 family has emerged. The different Bcl-2 pro-survival proteins have specific affinities for the various BH-3 only pro-death proteins (30, 31). While Bim and PUMA are capable of binding comparably to multiple pro-survival family members, Bad displays an affinity for Bcl-2, Bcl-x_L, and Bcl-w, while Noxa binds only to A1 and Mcl-1; these relationships are illustrated in Figure 1.3. This specificity of binding interactions will likely prove critical to the ongoing efforts to target the Bcl-2 family clinically using novel therapeutics.

Figure 1.2

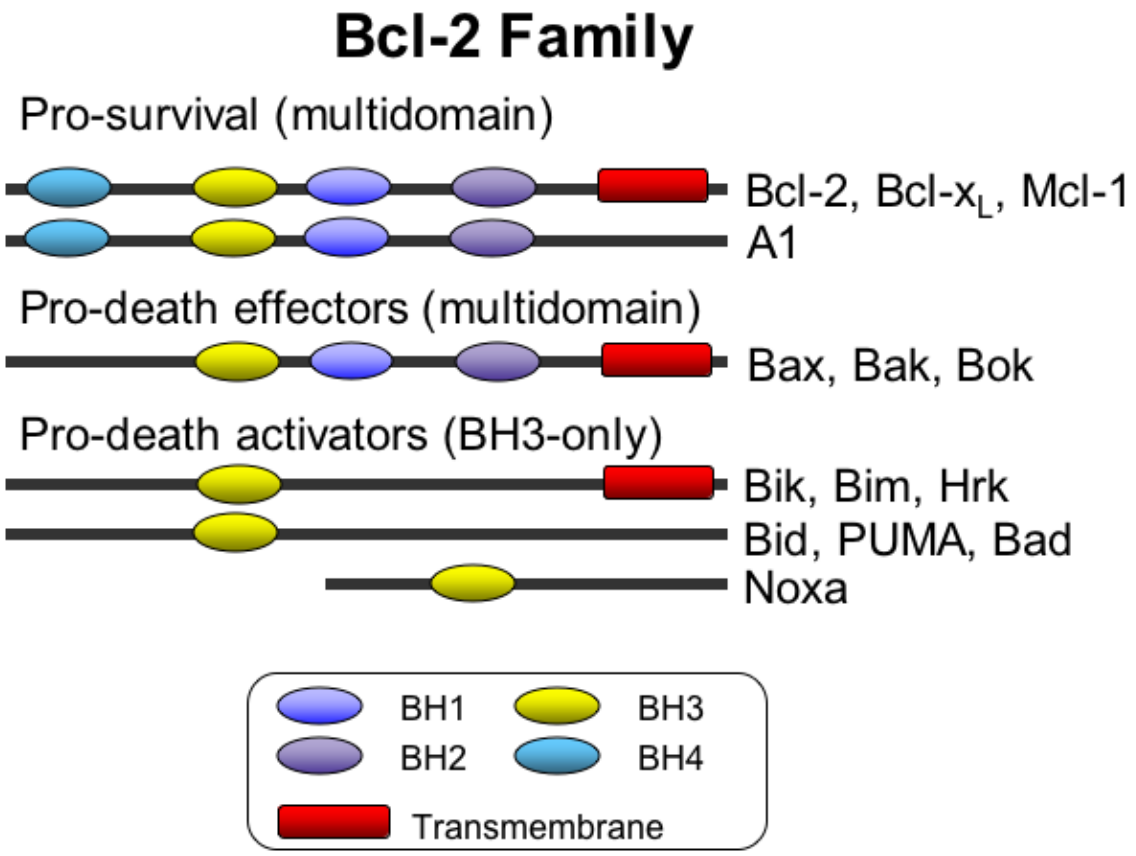

Figure 1.2 The mammalian Bcl-2 superfamily and sub-families. Bcl-2 family members contain at least one of 4 common Bcl-2 homology (BH) domains. Many members also include a hydrophobic domain near the C-terminus that allows for membrane anchorage. The multidomain pro-survival proteins contain all four BH domains, and most have a transmembrane domain. Pro-death effectors lack a BH4 domain, and are believed to be the determinants of mitochondrial apoptosis commitment, through pore formation in the mitochondrial outer membrane. The BH3-only proteins are the most diverse group, sharing only the BH3 homology domain. These proteins, which have distinct regulation patterns, act as initiators of apoptosis via binding to the pro-survival Bcl-2 proteins.

Figure 1.3

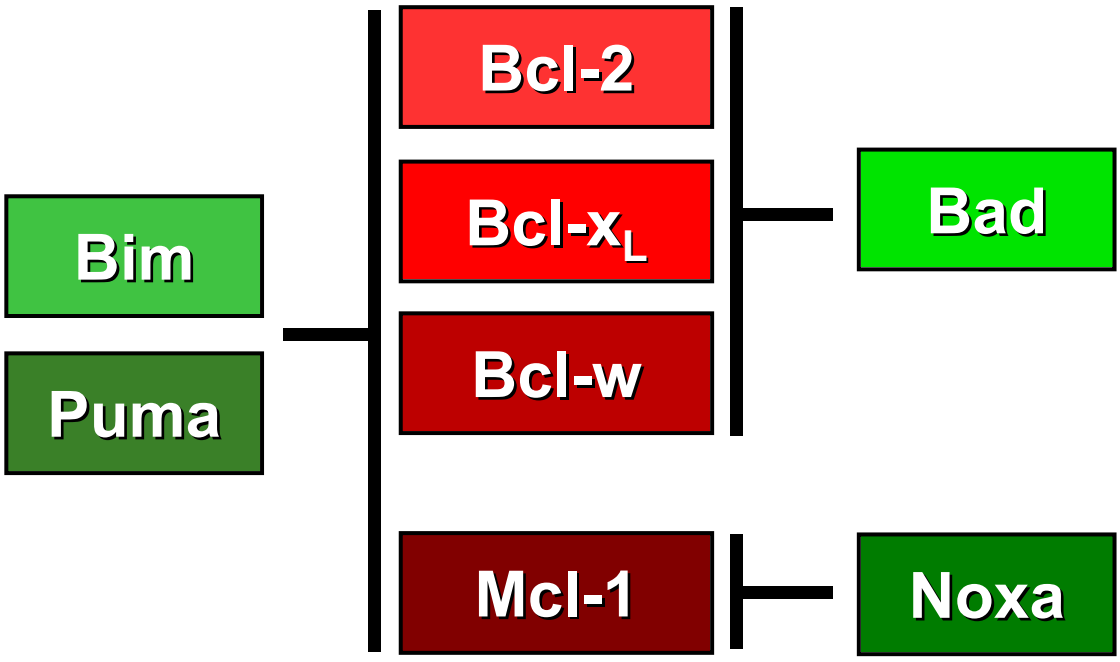

Figure 1.3 Schematic model of affinities between BH3-only pro-death proteins (in green) and multidomain pro-survival Bcl-2 proteins (in red). The interactions amongst the proteins are based on binding data. On the left are BH3-only proteins with broad, promiscuous binding patterns, while the BH-3 only proteins on the right show greater selectivity. Adapted from Chen et al., 2005 (30).

Bcl-2 Proteins and Cancer

The role of Bcl-2 family members in cancer is well established. In fact, the name of the prototypical family member, Bcl-2, is short for “B-cell lymphoma 2’, a reflection of the fact that this protein it is commonly upregulated following a translocation event in follicular B-cell lymphomas (32). Subsequently, mutations and dysregulations of the various Bcl-2 genes have been reported in wide range of cancers, and often are implicated in chemoresistance. Pro-survival Bcl-2 family members have been classified as oncogenes: when a broad panel of 1200 drugs was tested against the protein expression profiles of the NCI panel of 60 human cancer cell lines, Bcl-x_L was the protein whose expression level most strongly correlated with chemotherapy resistance (33). Conversely, the pro-death Bcl-2 proteins can act as tumor suppressors, and as such, the loss or mutation of their corresponding genes can contribute to tumorigenesis. For example, mutations in Bax and/or loss of Bax expression occurs in a significant subset of human cancers, particularly in lymphomas, leukemias, and colorectal cancers (34, 35); similar findings regarding Bak have been made in gastric and colorectal cancers (36). Mutations in BH3-only proteins have likewise been identified in a number of tumors, including adenocarcinomas (37, 38) and hematologic malignancies (39, 40).

The Bcl-2 Family and Melanoma

The pro-survival proteins Bcl-2, Bcl-x_L, and Mcl-1 have each been implicated for potential roles in melanoma progression. The association of Bcl-2

itself with melanoma is controversial; while it is accepted that Bcl-2 is a critical factor in melanocyte survival, publications have variously concluded that the levels of Bcl-2 increase, decrease, or have no correlation with aggression in melanomas (5, 41, 42). Furthermore, the initial favorable results reported for the treatment of melanoma with olblimersen, a Bcl-2 anti-sense oligonucleotide, were not sustained in a large phase III trial (43). The most recent data suggest that that higher Bcl-x_L and Mcl-1 levels more closely and consistently correspond to melanoma progression than Bcl-2 levels do (42, 44). Loss of expression of Bax and/or Bak, the pro-death effectors, has been shown to correlate with disease progression and chemoresistance in some, but not all melanomas (42, 45, 46). Bid, Bad, PUMA, and Noxa are among the BH-3 only proteins expressed in melanomas, but their specific roles in melanoma chemotherapy resistance have not been well studied previously. In Chapter II, I will explore the impact of blocking specific Bcl-2 proteins within the context of proteosomal inhibition, and will furthermore examine means of exploiting these findings to enhance melanoma responsiveness to this class of therapeutics.

Proteasomal Inhibition and Melanoma

The maintenance of protein homeostasis is a critical function within all cells, and it is no less so in cancer cells. In fact, because of their high proliferative rate, cancer cells require an efficient turnover of cellular components, in particular cell-cycle regulators. Thus, the control of protein degradation is a potential target for novel cancer therapies (47-49). In eukaryotic

cells, the primary intracellular cytosolic proteolytic system is the proteasome, a multi-catalytic complex which efficiently and selective degrades proteins marked for destruction by the covalent addition of ubiquitin chains. The ubiquitin-proteasome pathway is responsible for the processing of >80% of cellular proteins (50), and as such, it is a major regulator of protein half-life, and thus levels of individual proteins.

The 26S proteasome is composed of two major subunits: a 20S core subunit, with 3 pairs of distinct proteolytic sites, and a 19S regulatory subunit, which controls access to the catalytic core (51, 52). While a number of compounds with proteasomal inhibitory activity have been tested as anti-neoplastic agents, bortezomib, a boronic dipeptide, was the first selective and reversible inhibitor of the proteasome to be developed (53). Introduced shortly after the turn of the century, bortezomib was initially investigated for use against hematologic malignancies; it is FDA approved for use as a single agent in the treatment of multiple myeloma (54). Bortezomib exhibits anti-neoplastic activity against a range of cancer types, in large part via the induction of apoptosis (49). In preclinical investigations, bortezomib was highly selective against melanoma, both *in vivo* and *in vitro* (55-57). However, in clinical trials of metastatic melanoma patients, bortezomib was ineffective as a monotherapy (58). A crucial question, therefore, is how to improve the bortezomib's efficacy without inducing secondary toxicities.

Initial studies on the mechanism of action of bortezomib suggested it functioned to blunt NF-κB activity, by preventing the degradation of IκB, the NF-

κB inhibitor (59-61). This mechanism makes teleological sense, in that NF-κB is a multi-pathway survival mediator that is active in tumor development (61). However, subsequent data comparing bortezomib to a highly specific blocker of IκB degradation indicate that the obstruction of NF-κB activity is a relatively minor component of bortezomib's anti-neoplastic mechanism (62). While NF-κB inhibition may play a role, our group discovered that, at least in the case of melanoma, the BH3-only protein Noxa is a target of the proteasome, and a main effector of the antitumoral activity of bortezomib (56); these findings were independently confirmed (57). This discovery suggested that the intrinsic apoptotic cascade, and specifically the Bcl-2 pathway, might represent a critical mechanism for bortezomib cytotoxicity in cancer. Given the specificity of Noxa for interaction with Mcl-1, the pro-survival protein, investigation of the effect of bortezomib on this Bcl-2 family member was the next logical step. As described in Chapter II, bortezomib treatment leads to increased Mcl-1 levels in melanomas. This provided both an explanation for bortezomib's relatively inefficient killing of melanomas, and also an opportunity for rational combinational therapy to improve melanoma response to proteasome inhibition.

Autophagy: A New Pathway to Cancer Cell Death?

Restoring apoptotic competency to melanomas can delay melanoma growth, but to date no clinically significant regression has been reported with pro-apoptotic agents (63). Therefore, we reasoned that other mechanisms may be playing an important role in melanoma chemoresistance. We focused on autophagy, a program of "self cannibalism" that is generating intense interest amongst cancer biologists (64-66).

Autophagy is a lysosome-associated degradative process that eukaryotic cells employ to break down both damaged or unneeded organelles and also large protein aggregates. Much like the proteasome, autophagy is required, at a basal level, for the maintenance of cellular health. Autophagic activity can also be induced, either externally by nutrient deprivation, hypoxia, and other extracellular stressors, or internally by organelle damage or other disruptions in cellular homeostasis. In some settings, however, instead of serving as a protective response, autophagy can lead to a form of programmed cell death. This autophagic cell death, also known as "Type 2 cell death" (to differentiate from apoptosis, i.e. "Type 1 cell death") is associated with depletion of essential structures and organelles in the cell (67). The idea of an 'autophagic rheostat,' in which the ideal amount of cellular autophagy is neither too much nor too little, is illustrated in Figure 1.4. The mechanisms of autophagic death in eukaryotic cells are still being defined, and the molecular determinants of the pro and anti-survival roles of autophagy, particularly in melanoma, are unclear.

A number of distinct types of autophagy have been described, which mainly differ in their sites of action and degradation targets. The term ‘macroautophagy’ denotes a process that involves the enclosure of targets within a cytosolic double-membrane vesicle, termed an autophagosome, prior to fusion with lysosomes. In contrast, ‘microautophagy’ refers to events in which invaginations of the lysosomal membrane directly sequester targets, without autophagosome formation. Other, more specialized types of autophagy have been also described, such as chaperone-mediated autophagy, and piecemeal autophagy of the nucleus. Autophagy can be either selective or non-selective, and an autophagosome can include relatively large or small amounts of cytosol along with proteins and organelles. Additional descriptive terms have been introduced to refer to particular selective autophagic processes; e.g. ‘pexophagy’ for the selective degradation of peroxisomes, ‘mitophagy’ for the degradation of mitochondria, etc. At the present time, macroautophagy, in which a distinct autophagosome is formed prior to lysosomal involvement, is the focus of the majority of interest in the cancer biology field. Hereafter, ‘autophagy’ will be understood to refer to macroautophagy within this thesis.

Figure 1.4

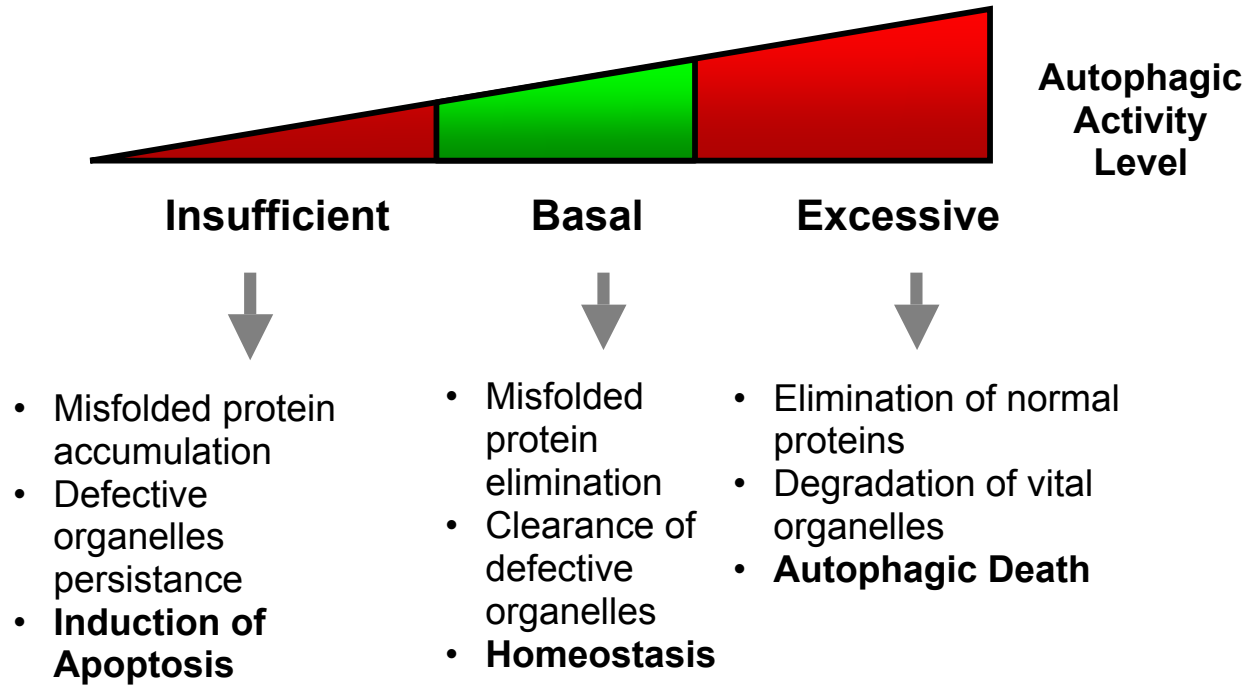

Figure 1.4 Concept of the rheostatic model of autophagy and cell fate. Autophagy is a process to clear damaged or unneeded organelles/proteins, and thus in healthy cells, it performs a vital function, particularly in response to stressors (center). In cells with insufficient autophagic function, the accumulation of damaged or defective structures leads to activation of apoptosis (left). In the opposite scenario, excessive autophagy can lead to a form of non-apoptotic programmed death, due to self-digestion of needed structures.

Mechanisms of Autophagy

Autophagy is a multistep process (please see Figure 1.5). Initially, a flattened membrane bilayer forms adjacent to the targeted organelle and/or cytosolic proteins. This stage is termed the *phagophore*, or alternatively an *isolation membrane*. Next, a cytoplasmic target is enveloped, and a closed, membrane-bound vacuole is formed, termed an *autophagosome*. A series of fusion events follow, resulting in maturation of the autophagosome. Initially, early endosomes and multivesicular endosomes fuse to the autophagosome; at this point, the vacuole is called an *amphisome*. Finally, fusion with lysosomes leads to a decrease in the luminal pH and activation of lysosomal hydrolases, which degrade the segregated material. At this last stage, the autophagic body is designated an *autolysosome*. Degradation products are then released into the cytosol, to be utilized for additional cellular functions (68, 69).

Concurrent with the above processes, a series of protein interactions and modifications occur that are required for autophagic cycling. The autophagy –related genes, or ATGs, encode a group of approximately 30 proteins that are well-conserved evolutionarily (70). While the details of the interactions between the Atg proteins have been worked out most precisely in yeast, the core mechanisms are retained within mammalian cells. This core machinery has 4 primary functional parts: 1) a regulated autophagy-induction complex; 2) an Atg9 cycling system for membrane recruitment; 3) a phosphatidylinositol 3-OH kinase (PI3K) complex driving amphisome nucleation, and 4) an ubiquitin-like protein system, which includes 2 interacting cascades of protein conjugations (70, 71).

Figure 1.5

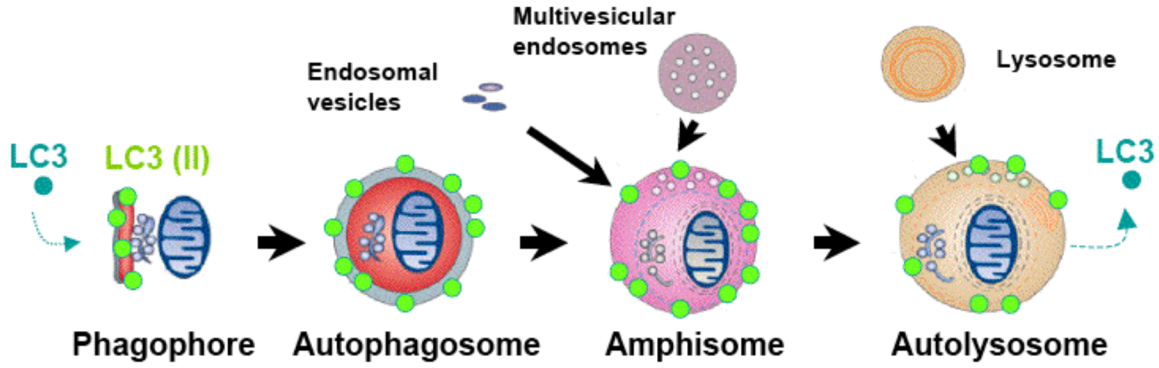

Figure 1.5 Stepwise pathway of macroautophagy. The initial step is formation of the phagophore, which is a lipid bilayer containing autophagy regulatory proteins. This structure grows to engulf cytoplasmic material and/or organelles, eventually enveloping targets in a double membrane layered structure termed an autophagosome, with degradation targets held inside the lumen. Maturation of the autophagosome follows, including fusion with multivesicular endosomes and/or endosomal vesicles, giving rise to multi-lamellar amphisomes. Fusion with lysosomes results in the import of lysomal enzymes as well as a decrease in pH, leading to degradation of the luminal contents within the mature autolysosome (also called an autolysophagosome). Once degraded, autolysosomal contents can be recycled for use by the cell.

The autophagy regulatory protein light chain 3 (LC3) is modified from its soluble state (LC3-I) by cleavage and C-terminal lipidation (LC3-II). The LC3-II form is incorporated into the phagophore outer membrane early in the pathway. It is maintained in autophagosomes until the resolution of the autolysosome, and thus, LC3 can be followed as a marker of autophagy. Figure adapted from Kroemer and Jäättelä, 2005 (64).

Initiation of Autophagy

Signals such as starvation that initiate autophagy in yeast inactivate TOR, the kinase responsible for regulating the formation of the initiation complex. The mammalian homologue of TOR, mTOR, appears to play a very similar role (72). The initiation steps of the autophagy cascade are detailed in Figure 1.6. The autophagy initiation complex includes Atg1, Atg13, and Atg17. Once mTOR is inactivated, ATG13 dephosphorylation leads to the induction complex formation. Atg9, a transmembrane protein, is the primary Atg protein responsible for recruiting membrane components to the nascent phagophore; it cycles between the phagophore and other cellular membrane reservoirs. A number of additional Atg proteins regulate the movement of Atg9 to and from the developing phagophore. The formation of the vesicular phagophore next requires a class III PI3K in complex with additional Atg proteins; in mammalian cells, this complex includes the PI3K Vps34, Vps15, and the Atg6 orthologue Beclin1 (73). This lipid kinase complex regulates the nucleation of the consolidating phagosome around its target.

Figure 1.6

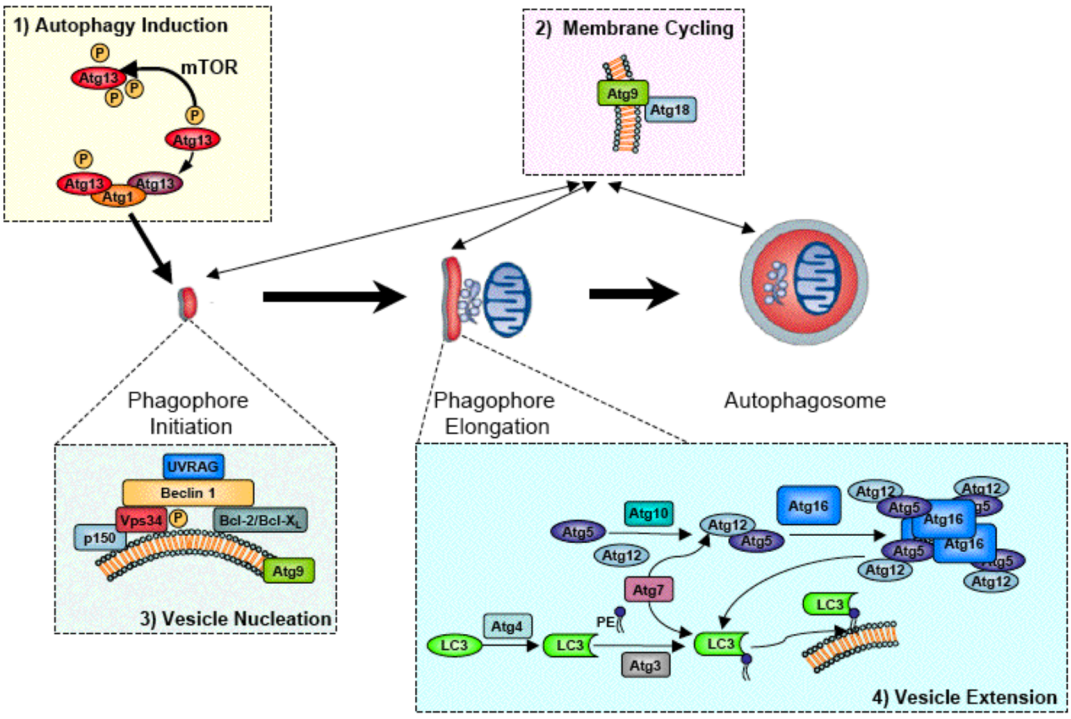

Figure 1.6 Autophagy regulatory steps: 1) Initiation of autophagy is regulated by mTOR; when mTOR is inactivated, Atg13 in dephosphorylated, and can associate with Atg1 and Atg17, leading to stimulation of Atg1 kinase activity and autophagy initiation. 2) Membrane cycling of Atg9 occurs throughout the process of autophagosome formation. 3) Vesicle nucleation involves the activation of Vsp34, a class III PI3-kinase, by phosphorylation; Vsp34 activity requires a complex that includes Beclin 1, p150, and UVRAG (UV radiation resistance-associated gene). 4) Vesicle elongation or extension is driven by two ubiquitin-like conjugation systems. The first involves covalent conjugation of Atg12 to Atg5, and requires Atg7 and Atg10. The second involves activation of LC3 via sequential action of the protease Atg4, and the conjugating enzymes Atg3 and Atg7, which add a phosphatidylethanolamine (PE) to LC3. This procession converts LC3 from the inactive LC3-I form to the active LC3-II form, leading to its association with autophagosomes. Figured derived in part from Legakis and Klionsky, 2006 (69); Maiuri et al, 2007 (74).

Autophagosome Maturation

Expansion of the phagosome into an autophagosome requires the ubiquitin-like (Ubl) proteins Atg8 and Atg12. Atg7, a protein with homology to the E1 ubiquitin activating enzyme, is required for the activation of both Atg8 and Atg12 (74). Atg12 is covalently conjugated to Atg5, and then forms a multimeric complex with other Atg proteins. Atg8 is cleaved by Atg4, and then conjugated to phosphatidylethanolamine (PE). This lipid conjugation shifts the soluble Atg8 to a membrane-bound form, localized in the phagosome. These complexes are believed to play a role in completion of the autophagosome and interaction with targets; however, Atg12-Atg5 complexes are not present in completed autophagosomes (75). Atg5, Atg7, Atg8 and Atg12 all have well-conserved orthologues in mammals; the mammalian Atg8 orthologue is microtubule-associated protein 1 light chain 3 (MAP1LC3), often called simply LC3 (76). The LC3 nomenclature is indicative of its lipid conjugation status: LC3 (I) represents unconjugated, soluble protein, whereas LC (II) is the activated PE-conjugated, membrane-bound form (77). Because Atg8/LC3 is maintained within the maturing autophagosome, it represents a useful marker of autophagosome formation, completion, and resolution.

Autophagosome Fusion Events and Resolution

The final steps in autophagy involve fusion with other lipid-bound structures (see Figure 1.6). Endosomes, some of which are organized as multivesicular complexes, fuse with autophagosomes, giving rise to amphisomes.

The purpose of endosomal fusion is postulated to involve the delivery of proteins required for amphisome fusion with lysosomes (78); however, the direct fusion of autophagosomes and lysosomes, without the amphisomal intermediate step, has also been described (79, 80). When the fusion with lysosomes takes place, the inner membrane of the autophagosome and the cytoplasm-derived materials within are degraded by lysosomal hydrolases. Once macromolecules have been degraded in the autophagolysosome, amino acids are exported back to the cytosol for cellular reuse.

Autophagy and Cancer

Why is autophagy of interest to cancer biologists? Several lines of evidence support a role for autophagy in cancer. First, autophagy proteins can function as tumor suppressors. For example, expression of *Beclin 1,* the orthologue of *Atg6*, is often lost in breast, ovarian and prostate cancers (81); mice heterozygous for *Beclin 1* loss develop a variety of tumors (82). Reintroduction of Beclin 1 expression to cancer cells lacking it inhibits proliferation and tumorigenesis (81). Other autophagy genes, such as *Atg8* and *Atg7,* are likewise deleted in a range of cancers (83-87). Autophagy genes can also play roles in the induction of cell death. For example, in *Bax-/Bak-* fibroblasts, which are defective for apoptosis, DNA damage induced by etoposide leads to cell death by autophagy. The knockdown of Atg5, Atg7, or Beclin 1 in these cells resulted in inhibition of cell death in response to etoposide treatment.

Taken together, these data suggest a model in which autophagy broadly functions as a tumor suppression mechanism (88).

Other data, however, support an opposite role for autophagy, one favoring tumor progression. The inactivation of *Atg5* with shRNA can lead to more rapid cancer cell death in response to chemotherapy or direct p53 activation (89). When immortalized *Bax-/Bak-* bone marrow cells are deprived of growth factors, instead of undergoing apoptosis, they enter into a prolonged, catabolic state of autophagy that does not result in cell death. Furthermore, when autophagy is blocked in this context, either genetically by knockdown of Atg5 or Atg7, or pharmacologically via the chemical autophagy inhibitors chloroquine or 3-methyladenine, the cells do die, quite rapidly (72). Additionally, when HeLa or HCT116 cancer cells are deprived of nutrients, autophagy is rapidly upregulated. Blockade of autophagy, either by genetic or pharmacologic means, results in apoptosis and cell death; this death can be delayed by additional Bax/Bak knockdown or caspase inhibition (90, 91). Thus, in these experiments, autophagy seems to function as a survival mechanism for cells in response to stressors. This is consistent with the generalized finding of high levels of autophagy in various cancer types (65).

In summary, the relationship between apoptosis and autophagy is complex. Similar stimuli can induce autophagy or apoptosis (or, more rarely, both) depending on the context (74), (see putative points of crosstalk in Figure 1.7) Autophagy and apoptosis share the ability to kill cells in certain circumstances;

autophagy, however, can also potentially serve as survival mechanism by which cells avoid stress-mediated death (66).

Autophagy and Melanoma

Little research has been done looking at autophagy specifically in melanoma. While it has been noted that many melanomas have a large number of autophagosomes in their cytosol, the significance of this finding is unknown (92). Our interest in autophagy was stimulated by the observation of autophagosome formation in melanoma cells in culture in response to chemotherapeutic treatment, in particular with the drug cyclopamine. In Chapters 3 and 4, I will discuss these findings in depth, as well as examine the potential implications for the treatment of this deadly disease.

Figure 1.7

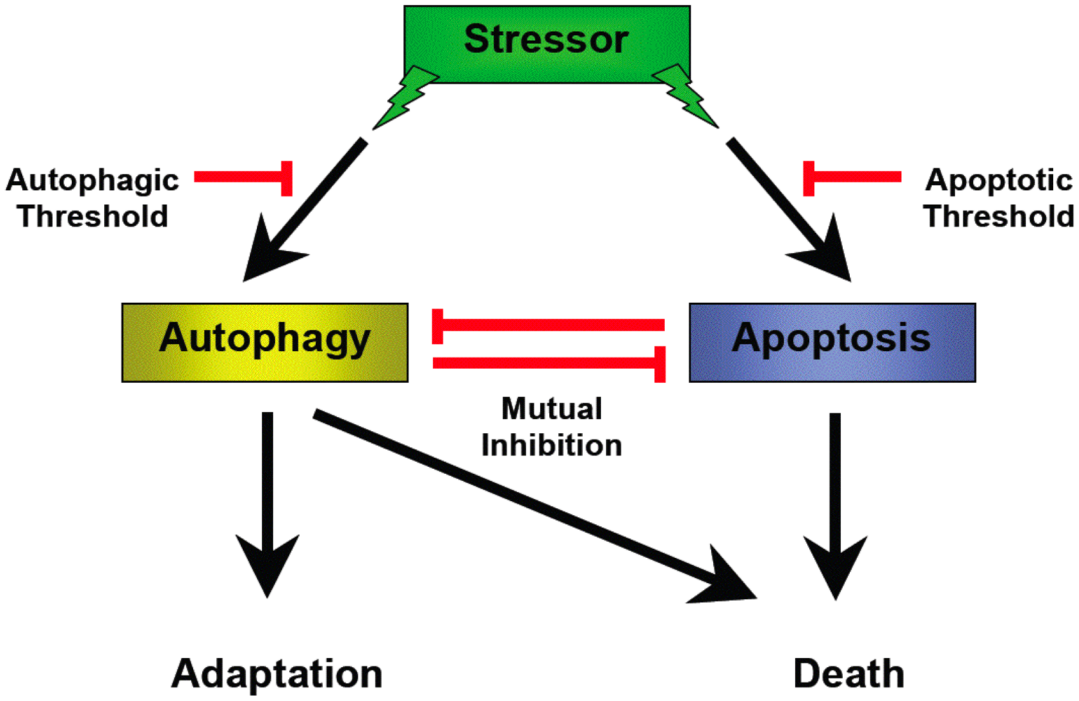

Figure 1.7 Relationship between apoptosis and autophagy. Cellular stressors can induce cells to undergo either apoptosis or autophagy, dependant upon context. The two processes exhibit some degree of mutual inhibition. While apoptosis exclusively leads to cell death, autophagy can be either adaptive or destructive. Figure adapted from Maiuri et al, 2007 (74).

CHAPTER II

Therapeutic Window for Melanoma Treatment Provided By Selective Effects of the Proteasome on Bcl-2 Proteins

Abstract

Melanoma cells depend on sustained proteasomal function for survival. However, at bioavailable doses, bortezomib, the first selective proteasome inhibitor in clinical use, is not sufficient to improve the poor prognosis of metastatic melanoma patients. Since the proteasome is expressed in both normal and tumor cells, it is unclear how to enhance the efficacy of bortezomib without exacerbating its secondary toxicity. In this chapter, I present pharmacological and genetic analyses of mechanisms of resistance to proteasome inhibition. We focused on Bcl-2, Bcl-x_L and Mcl-1 as the primary anti-apoptotic factors associated with melanoma progression. We found that bortezomib could not counteract the intrinsically high levels of Bcl-2 and Bcl-x_L in aggressive melanoma cells. Moreover, Mcl-1 was only downregulated once the apoptotic machinery was activated. Based on these results, a combination treatment containing bortezomib and (-)-gossypol, an inhibitor of Mcl-1, Bcl-2, and Bcl-x_L, was designed and proven effective *in vivo*. Using a specific RNA interference approach, we found a hierarchical impact of anti-apoptotic Bcl-2 family members on the resistance to bortezomib. Thus, melanoma cell survival after proteasome inhibition relied primarily on Mcl-1, and to a lesser extent on

Bcl-x_L. However, Bcl-2 played a dispensable role. Importantly, under equivalent conditions, neither Mcl-1 nor Bcl-x_L inactivation affected the viability of normal melanocytes. These differential roles of Bcl-2 family members in normal and malignant cells offer a window for therapeutic intervention that can be exploited to overcome melanoma chemoresistance in a tumor cell-selective manner.

Introduction

As discussed above, metastatic melanoma remains a daunting clinical problem. Incidence continues to rise, and the prognosis for patients at late stages of the disease has not significantly improved in the last three decades (93, 94). However, recent discoveries elucidating the molecular biology of metastatic melanoma have led to optimism about the rational design of more effective treatments (23, 95). The proteasome is one such attractive target for cancer therapeutics. We and others have previously shown that in experimental models, melanoma cells are highly dependent on proteasomal function for survival (55-57, 96, 97). Thus, bortezomib, the prototype of selective proteasome inhibitors currently in clinical trials (49, 50), can compromise the viability of a spectrum of melanoma cells (i.e. from early, intermediate and late stages of the disease) (56).

Genetic and functional studies in melanoma and other cancers have unveiled the critical role of the pro-apoptotic protein Noxa in the response to proteasome inhibition (56, 57, 97-99). Recent studies suggest that the main function of Noxa is to promote cell death by “neutralizing” anti-apoptotic factors, particularly Mcl-1 (30, 100-102), ultimately promoting the release of apoptogenic factors from the mitochondria (see ref (30) for a recent review). However, although Noxa increase is an early result of bortezomib treatment, the execution of cell death can be substantially delayed. While a 5 to 20-fold accumulation of Noxa can be visualized as early as 6 hours post-treatment with bortezomib, caspase activation may not be detected until 12-48 hours later (56). Therefore, melanoma cells seemingly retain anti-apoptotic signals that counteract

proteasome inhibition and Noxa upregulation. Noxa-independent mechanisms of resistance are likely also to exist since Noxa is not the sole mediator of the response of tumor cells to proteasome blockade (56, 96). Understanding how normal and tumor cells activate survival pathways to compensate for proteasome inhibition may be important *in vivo*. In melanoma xenograft models, bortezomib can act as a sensitizer to other chemotherapeutics, but is not able to effect a significant response as a single agent (55, 56, 97). In a recent clinical trial, bortezomib failed to provide significant therapeutic benefit to patients with metastatic melanoma (58).

The development of treatments tailored to enhance the efficacy of bortezomib without increasing secondary toxicity has been complicated by a lack of consensus regarding the impact of proteasome inhibition on the apoptotic machinery. Mcl-1 levels accumulate in response to bortezomib (56, 57, 97), but Mcl-1 is also cleaved by caspases once apoptosis is induced (56, 103). Interestingly, partial downregulation of Mcl-1 was shown to cause a two-fold increase in bortezomib-mediated melanoma killing in culture (97). The question of how to efficiently block Mcl-1 *in vivo* without increasing the toxicity to normal cells remains. The relative contribution of other Bcl-2 family members to normal and tumor cell maintenance upon bortezomib treatment is also not clear. Thus, Bcl-2, Bcl-x_L, and Bax, have variously been demonstrated to be either unaffected by bortezomib, downregulated before the activation of the apoptotic machinery, or inhibited after caspases are processed (49, 50, 104) depending on the tumor type examined.

Small molecule inhibitors of anti-apoptotic Bcl-2 proteins are emerging as potent tools to address functional components of the apoptotic machinery, with the ultimate objective of overcoming tumor chemoresistance (102, 105, 106). Significant effort has been dedicated to the design of compounds that mimic the BH3 domain of pro-death Bcl-2 proteins (105, 107). ABT-737, which is the best characterized BH3 mimetic to date (108), was found to synergize with compounds such as dexamethasone or paclitaxel in assays of *in vitro* killing of multiple myeloma cells. However, ABT-737 had only a relatively modest effect on the cytotoxicity of bortezomib (1.3 fold induction) (109). ABT-737 has a high affinity for Bcl-2 and Bcl-x_L, but binds poorly to Mcl-1 (108). Broader spectrum antagonists of anti-apoptotic Bcl-2 proteins are being investigated [recently reviewed in (107)]. These include the natural products or derivatives of epigallocatechin gallate (EGCG), gossypol, antimycin A and chelerythrine; as well as synthetic compounds GX-15, BH3I-1 and YC-137. Among these agents, the lowest IC_{50} values for Mcl-1 have been reported for EGCG and gossypol (0.92 and 1.75 μM, respectively). Gossypol is interesting because to our knowledge, it is the only bioavailable compound able to bind Mcl-1 (110) that is in being tested in Phase II clinical trials as a BH3 mimetic (111). In the context of melanoma, gossypol is relevant because it has long been known to kill melanoma cells with a higher efficacy than normal melanocytes (112-115). However the mechanism(s) underlying this selectivity is unclear.

Here we report an analysis of mechanisms of cell survival in melanoma cells and normal melanocytes with blocked proteasomal functions. We combine

genetic and pharmacological approaches (based on RNA interference and gossypol, respectively) to address the impact of targeting specific Bcl-2 family members on the response to bortezomib *in vitro* and *in vivo*. We show that the regulation and functional requirement of Bcl-2, Bcl-x_L and Mcl-1 are not equivalent in melanoma cells *versus* normal melanocytes. Moreover, melanoma cells, but not melanocytes, require Mcl-1 and Bcl-x_L for survival if the proteasome is blocked. This study provides new insight into the relationship between the proteasome and the apoptotic machinery in melanoma, which could be exploited to design more effective and selective therapies.

Results

Identification of protective signals opposing bortezomib in melanoma cells

To address mechanisms of melanoma resistance to bortezomib, SK-Mel-19, SK-Mel-103 and SK-Mel-147 were chosen as representative examples of well-characterized metastatic melanoma cell lines that respond to bortezomib by undergoing programmed cell death (56, 96). Consistent with previous reports (56, 96), bortezomib induced Noxa in all three cell lines, but this drug was not rapidly cytotoxic (Figure 2.1). Noxa could be detected as early as 4 h after treatment, achieving a maximum level at 12-14 h. However, an average of 56 h, 30 h and 36 h were needed to induce > 75% cell death in SK-Mel-19, -103 and -147 lines, respectively (Figure 2.1a-c).

Peptide-based assays have demonstrated that Noxa has higher affinity for Mcl-1 than for other anti-apoptotic Bcl-2 proteins (30, 31). In fact, recent studies have demonstrated Noxa binding to Mcl-1 in melanoma (97). Bcl-2 and Bcl-x_L may also be relevant because they may bind to the high Noxa levels induced by bortezomib treatment, and/or block Noxa-independent death programs (30, 101, 102). Cells were collected at different time points following bortezomib treatment, and the expression of Noxa, Mcl-1, Bcl-x_L and Bcl-2 visualized by immunoblotting. Processing of regulatory caspases (Casp-9 and -8) and effector caspases (Casp-3 and -7) was monitored, as a reference for the activation of classical apoptotic mediators.

As shown in Figure 2.1a-c, in all analyzed melanoma cell lines, Mcl-1 protein levels rapidly increased following bortezomib treatment. A 2-2.5 fold Mcl-

1 induction was detectable within 1 h of incubation with bortezomib, preceding the accumulation of Noxa (see quantification of relative induction of the two proteins in Figure 2.1a-c; visualization of the early induction of Mcl-1 in the insets; and the accumulation of Noxa and Mcl-1 in Figure 2.1d-f). Note that significant cell death was not achieved until the regulatory and effector caspases became activated, and Mcl-1 expression was reduced to or below basal levels (Figure 1d-f). Bcl-2 and Bcl-x_L expression remained high during treatment, and did not change upon caspase activation. These results emphasize the differential regulation of Bcl-2 family members by the proteasome, and suggest that the idiosyncratic rate of synthesis and accumulation of Mcl-1 may serve as an internal brake opposing the toxicity of proteasomal inhibition.

Figure 2.1 Impact of bortezomib on regulators and effectors of programmed cell death. (a–c) Comparative analysis of cell death (white circles) and accumulation of NOXA and Mcl-1 (black circles and black squares, respectively), in SK-Mel-19 **(a)**, SK-Mel-103 **(b)** and SK-Mel-147 **(c)** induced by 50 nM bortezomib in standard culture conditions. Cell death was determined by trypan blue exclusion assay. **(d–f)** Early induction of NOXA, but delayed caspase processing in melanoma cells treated with bortezomib estimated by protein immunoblotting. Tubulin is used as a loading control. Arrows point to processed caspases. In this, and other figure legends, NT stands for cells treated with vehicle control (0.025% DMSO)**.**

Figure 2.1

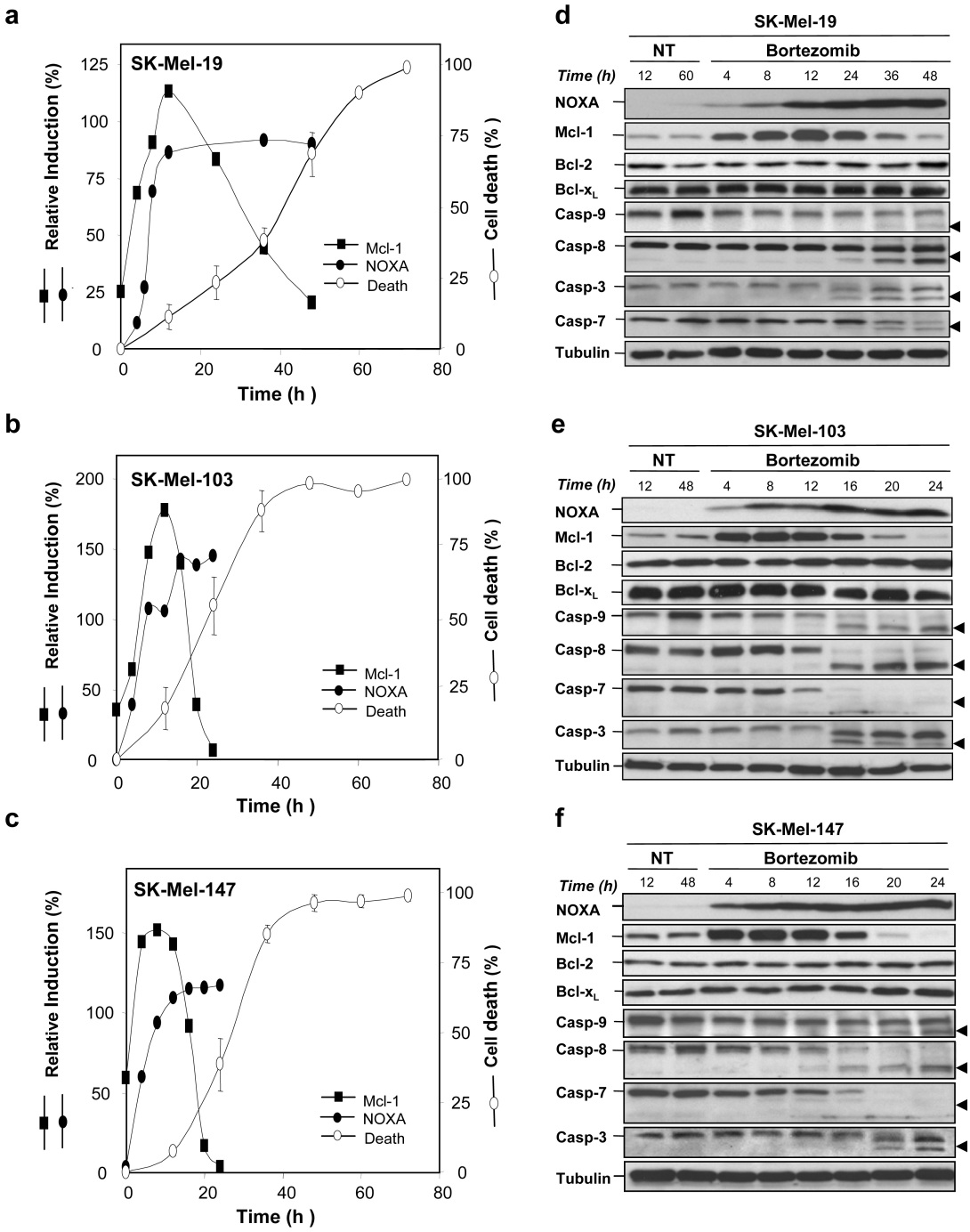
a
SK-Mel-19
Relative Induction (%)
Cell death (%)
Time (h)
Mcl-1
NOXA
Death
b
SK-Mel-103
c
SK-Mel-147
d
SK-Mel-19
NT
Bortezomib
Time (h)
12 60 4 8 12 24 36 48
NOXA
Mcl-1
Bcl-2
Bcl-xL
Casp-9
Casp-8
Casp-3
Casp-7
Tubulin
e
SK-Mel-103
12 48 4 8 12 16 20 24
f
SK-Mel-147

Multi-target BH3 mimetics to improve of the efficacy of bortezomib

Given sustained levels of Bcl-2 and Bcl-x_L, and massive induction of Mcl-1 by bortezomib, blocking these three anti-apoptotic proteins may improve the efficacy of proteasome inhibition *in vivo*. As indicated above, we focused on gossypol as a representative bioavailable compound with known BH3 function, one which had been shown in clinical trials to have a safe profile (110).

Natural gossypol (a mixture of (-) and (+) enantiomers) binds Mcl-1, Bcl-2 and Bcl-x_L with IC_{50} values of 1.74 μM, 0.28 μM and 3.03 μM, respectively (107). However, a number of reports have shown that of the two enantiomers, (-)-gossypol has significantly more anti-cancer activity *in vitro* and *in vivo* (see Ref (110) for review). To estimate the binding affinities (-)-gossypol for individual Bcl-2 family members, competitive polarization assays were performed with a fluorescently tagged Bid BH3 peptide (111) (see Materials and Methods). *K*i values, instead of binding concentrations, were determined, as they more directly measure the inhibitory capacity of (-)-gossypol. As shown in Figure 2.2a, the *K*i of (-)-gossypol for Mcl-1, Bcl-2 and Bcl-x_L were 180 nM, 320 nM and 480 nM, respectively. Specific binding of (-)-gossypol to its targets was validated by fluorescence resonance energy transfer. Because of its high affinity for Mcl-1, we focused on the (-) enantiomer of gossypol for studies of melanoma resistance to bortezomib.

When combined with bortezomib *in vitro*, (-)-gossypol selectively enhanced melanoma killing. As shown in Figure 2.2b, the addition of (-)-

gossypol at 1μM increased cell killing in all melanoma cell lines tested. Human primary melanocytes remained viable upon adding (-)-gossypol to bortezomib (Fig. 2.2b, see also Fig. 2.2c for representative microphotographs). These data suggest a tumor-restricted cooperativity between (-)-gossypol and proteosomal inhibition.

Figure 2.2 (-)-Gossypol, a BH3 mimetic, augments bortezomib-mediated melanoma cell killing in vitro. (a) Estimation of inhibitory constants (Ki). Inhibition of Bcl-2, Bcl-x_L and Mcl-1 proteins in vitro, based on fluorescence polarization in a competitive binding assay using a fluorescently labeled peptide corresponding to the BH3 domain of Bim (FAM-Bid-BH3). Values for Bcl-2, Bcl-x_L or Mcl-1 protein bound to FAM-Bid-BH3 in the absence of gossypol defined the maximal fluorescence polarization (0% inhibition). The molecular structure of gossypol is shown in the inset. Binding affinities correspond to Ki values (μM) for the indicated Bcl-2 family members. **(b)** The effect of (-)-gossypol and bortezomib, as single agents or combination, against foreskin melanocytes and a panel of melanoma cell lines in culture. Cells were treated with 10 nM bortezomib (Bor) and/or 1 mM (-)-gossypol (Gos), for 36 h, and cell death was assessed by trypan blue exclusion. **(c)** Representative micrographs of the indicated cell populations treated as in **(b)**. Note the lack of effect of the bortezomib/(-)-gossypol combination on the morphology or cell density of normal melanocytes.

Figure 2.2

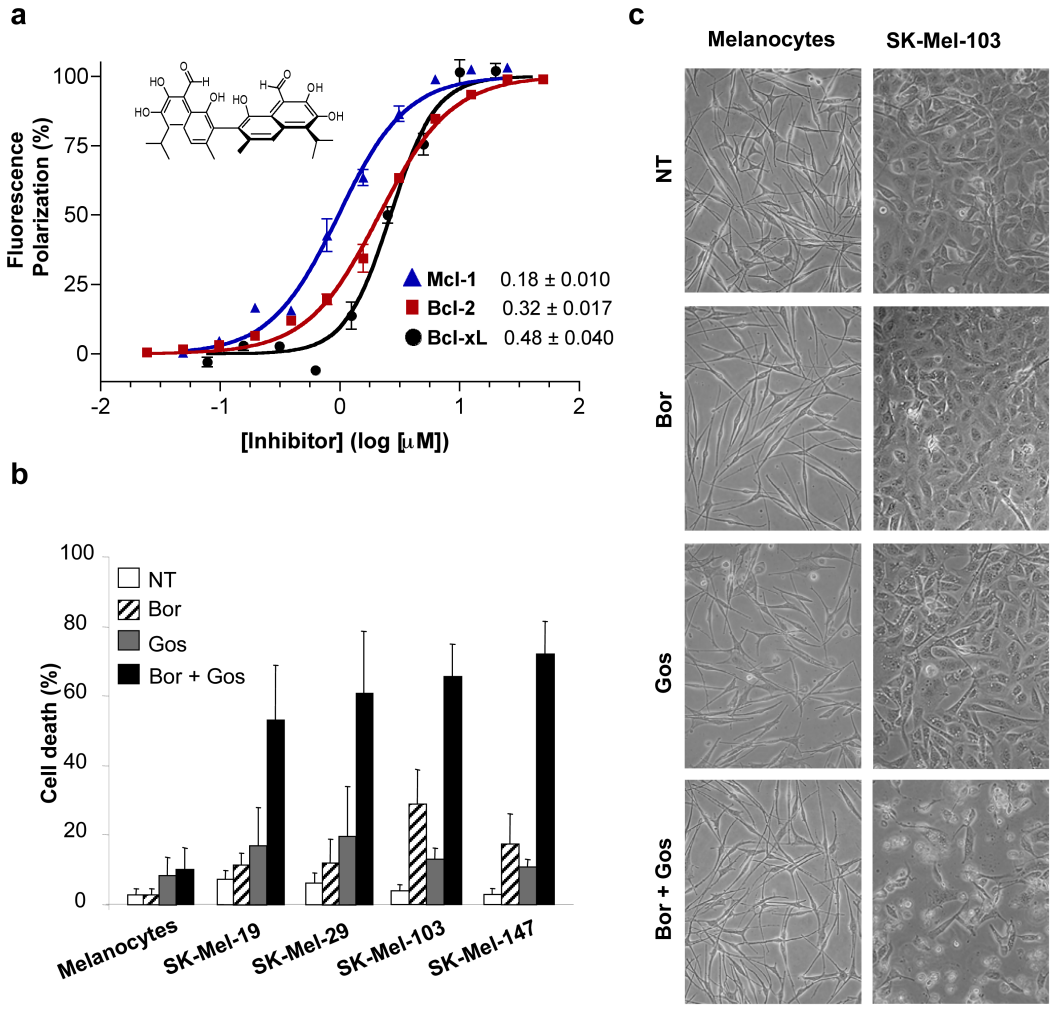
a
Fluorescence Polarization (%)
100
75
50
25
0
-2
-1
0
1
2
[Inhibitor] (log [μM])
Mcl-1 0.18 ± 0.010
Bcl-2 0.32 ± 0.017
Bcl-xL 0.48 ± 0.040
b
Cell death (%)
100
80
60
40
20
0
NT
Bor
Gos
Bor + Gos
Melanocytes
SK-Mel-19
SK-Mel-29
SK-Mel-103
SK-Mel-147
c
Melanocytes
SK-Mel-103
NT
Bor
Gos
Bor + Gos

Anti-tumor effect of the (-)-gossypol/bortezomib combination *in vivo*

We have previously shown that, among a panel of 19 melanoma lines, the SK-Mel-103 and SK-Mel-147 lines grow most aggressively in immunosuppressed mice (56). In addition to expressing high levels of Mcl-1, Bcl-2, and Bcl-x_L (Figure 1e-f), SK-Mel-103 and SK-Mel-147 are resistant to DNA damaging agents and other chemotherapeutic drugs currently being tested in preclinical settings, such as inhibitors of the MAPK pathway (116, 117). Therefore, these two cell lines were selected for treatment assays *in vivo.*

To enable non-invasive tumor visualization, both melanoma lines were infected with retroviral vectors encoding GFP. Melanoma cells were implanted subcutaneously (s.c.) to generate localized xenografts, or intravenously (i.v.) to induce disseminated tumors. Treatment was initiated once tumor cells started to proliferate actively (48 h after the s.c. implantations), or implant in the lungs of recipient mice (72 h after the i.v. injections) (56). Bortezomib and (-)-gossypol were administered systemically at concentrations below their described maximum tolerated dose (see Materials and Methods).

Bortezomib was able to reduce growth of SK-Mel-103 s.c. xenografts (see representative examples in Figure 2.3a and quantification in Figure 2.3b). However, as previously described (56), this effect was not statistically significant (p=0.190). Tumor growth was also delayed by (-)-gossypol (p=0.043). However, the combination of (-)-gossypol and bortezomib was significantly more potent than each agent alone (p=0.005; Figure 2.3a, b).

Figure 2.3 Gossypol augments the antitumor effect of bortezomib against melanoma *in vivo*. (a) Photographs of mice inoculated s.c. with GFP-tagged SK-Mel-103 and imaged with visible light (upper panels) or by fluorescence imaging (bottom panels) at day 17 of treatment with placebo control, bortezomib (Bor), (-)-gossypol (Gos) or a combination of both agents. Quantification of tumor growth is shown in **(b)**. **(c)** Analysis of the impact of (-)-gossypol and bortezomib, as single agents or combination in a surrogate model of melanoma metastasis. Indicated is the number of metastatic lung nodules ≥ 2mm in diameter observed at day 17 post treatment in mice inoculated i.v. with SK-Mel-103 or SK-Mel-147. **(d)** Representative fluorescence photographs of lungs from animals inoculated with SK-Mel-103 or SK-Mel-147, and treated with the indicated compounds. Note the reduced number and size of tumor nodules provided by the bortezomib/(-)-gossypol combination.

Figure 2.3

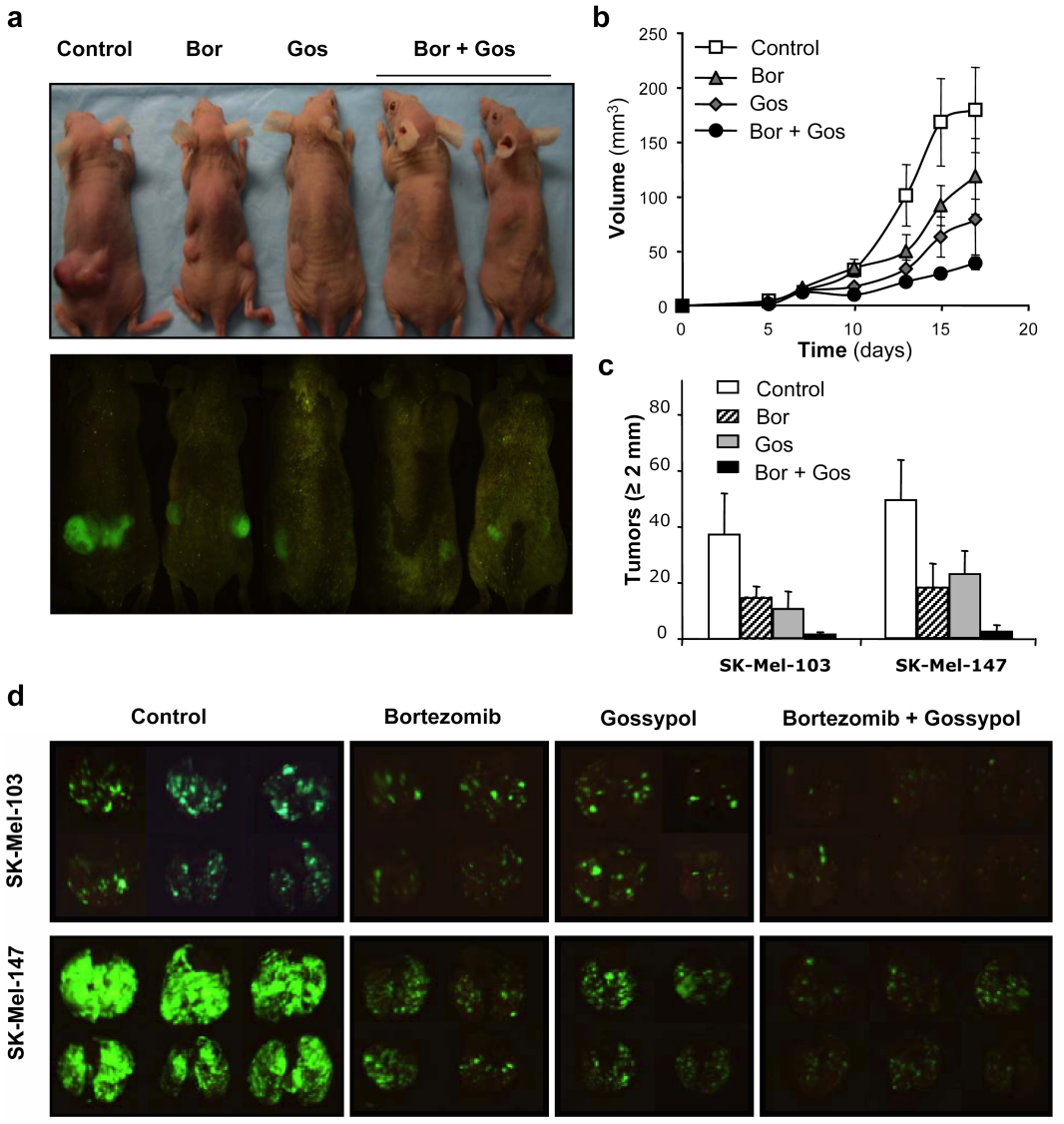
a
Control
Bor
Gos
Bor + Gos
b
Control
Bor
Gos
Bor + Gos
Volume (mm3)
Time (days)
c
Control
Bor
Gos
Bor + Gos
Tumors (≥ 2 mm)
SK-Mel-103
SK-Mel-147
d
Control
Bortezomib
Gossypol
Bortezomib + Gossypol
SK-Mel-103
SK-Mel-147

While these results are encouraging, the impact of the drug combinations on the control of metastatic dissemination is perhaps more relevant, since metastasis is the leading cause of death in melanoma patients (23, 94, 95). Interestingly, the (-)-gossypol/bortezomib combination provided a significant reduction in the metastatic dissemination of SK-Mel-103 and SK-Mel-147 (Figure 2.3c,d). Consequently, the anti-tumor effect of bortezomib/(-)-gossypol improved overall survival. By day 17 after treatment, more than 70% of control mice treated with placebo had either died or were moribund as result of significant respiratory complications. In contrast, no deaths were detected in the (-)-gossypol/bortezomib combination at that time, and these mice showed no signs of discomfort. Macroscopic analyses of lungs mice implanted with cell line SK-Mel-147 revealed a reduced size and number of metastatic nodules after treatment with both drugs (Figs. 2.3c,d). The average number of metastatic lung nodules ≥ 2 mm diameter was 50, 16, and 20 per mouse, in animals treated with placebo control, bortezomib or (-)-gossypol as single agents, respectively (Figure 2.3c.) However, only an average of 3 metastases ≥2 mm were detected per mouse in the group treated with the bortezomib/(-)-gossypol combination (p=0.001; see representative examples of lungs visualized by fluorescence-based imaging systems in Figure 2.3d). The impact of the drug combination was also evident, though less pronounced, in SK-Mel-103 (Figure 2.3c,d and results not shown). Importantly, the anti-melanoma activity of the (-)-gossypol/bortezomib combination was not associated with noticeable secondary

toxicity. Given the traditional poor efficacy of conventional chemotherapeutic agents, our results could have important translational implications.

Genetic analysis of the contribution of anti-apoptotic Bcl-2 proteins to tumor cell survival after proteasomal inhibition: RNA interference

As indicated above, a variety of biochemical and mechanistic analyses in multiple cancer types have provided ample support for the anti-tumoral effect of (-)-gossypol, primarily linked to its role as a BH3 mimetic. However, dysregulation of mitochondrial and redox-dependent functions by gossypol can affect, directly or indirectly, other cellular processes (110) that may act in a BAX/BAK independent manner (118). Therefore, an independent genetic approach based on highly specific RNA interference was developed to validate the BH3-dependent function of (-)-gossypol and establish the hierarchical requirement of Bcl-2 family members for cell viability upon bortezomib treatment. Specifically, short hairpins RNAs (shRNAs) against unique regions of Mcl-1, Bcl-x_L or Bcl-2 were cloned into a lentiviral vector under control of the H1 promoter (Figure 2.4a; see Materials and Methods and Ref. (119) for additional information). The vector expresses eGFP under an independent promoter (UbiC) for titer quantification and imaging of transduced cells. As shown in Figure 2.4b, this approach allowed for a nearly complete infection of melanocytes and melanoma cells (i.e. > 95% cells can be visualized as GFP positive within two days after infection). The efficacy and selectivity of this approach is shown in Figure 2.4c. A reduction of > 90% for Mcl-1, Bcl-x_L or Bcl-2 could be achieved

without an apparent effect on the expression of other Bcl-2 homologue proteins (i.e. the shRNA construct against Mcl-1 does not affect Bcl-2 or Bcl-x_L levels, and vice versa; Figure 2.4c).

Figure 2.4 Specific knockdown of Bcl-2 family members by highly efficient and selective lentiviral-driven shRNA. (a) Schematic representation of the lentiviral vector used for RNA interference. shRNA is driven by the H1 RNA promoter and the reporter GFP by the ubiquitin-C promoter. The 5' positions of the 19 bp sequences of human *Bcl-2*, *Bcl-x_L*, and *Mcl-1* targeted by the shRNAs, are listed on the right. **(b)** Brightfield and fluorescence photomicrographs of primary human melanocytes or SK-Mel-103 melanoma cells infected with the shRNA lentiviral constructs, or a control construct encoding a scrambled sequence. The high infection efficiency was evidenced by > 90% GFP positive cells. **(c)** PAGE-SDS immunoblotting demonstrating the efficacy and selectivity of Bcl-2, Bcl-x_L or Mcl-1 downregulation. Actin is shown as a loading control.

Figure 2.4

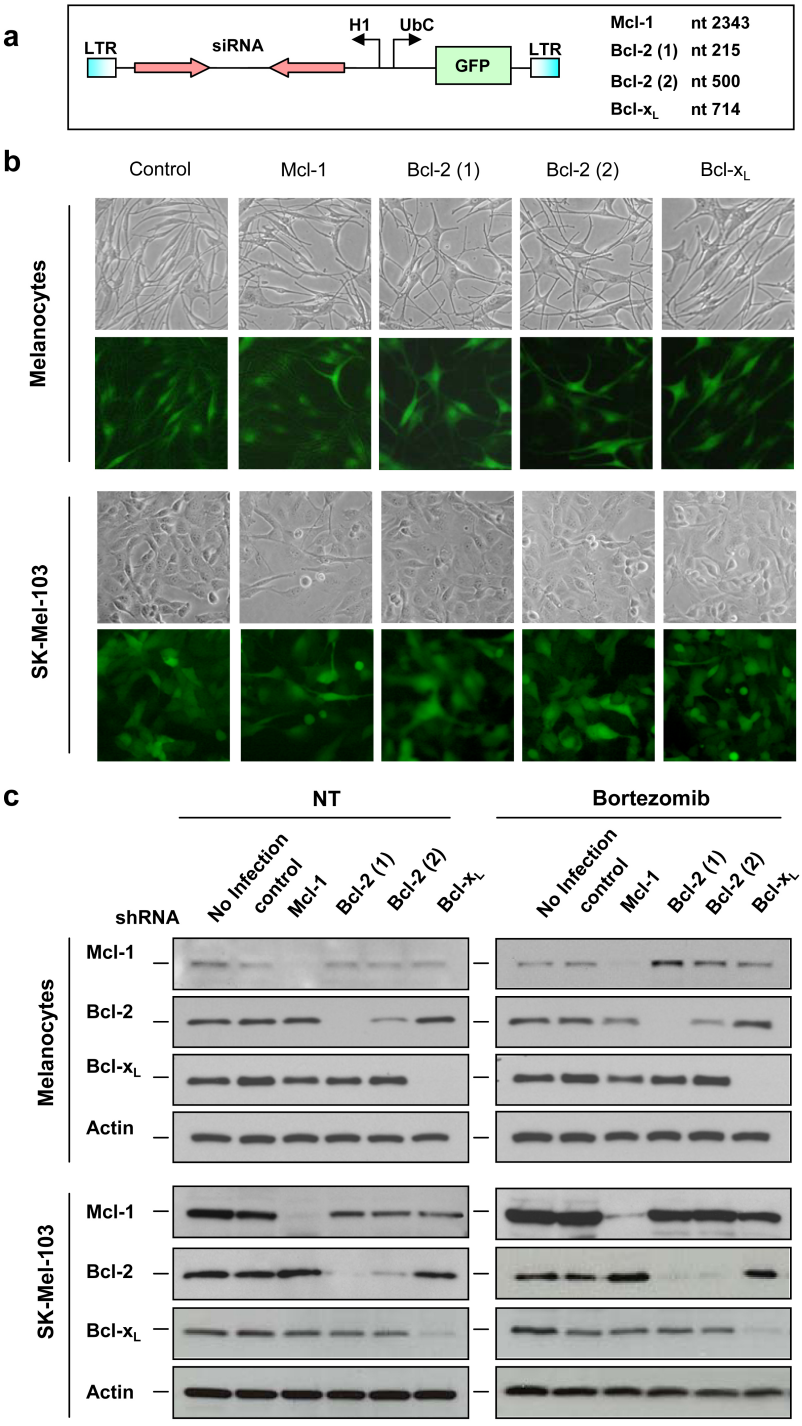
a
LTR
siRNA
H1
UbC
GFP
LTR
Mcl-1 nt 2343
Bcl-2 (1) nt 215
Bcl-2 (2) nt 500
Bcl-xL nt 714
b
Control
Mcl-1
Bcl-2 (1)
Bcl-2 (2)
Bcl-xL
Melanocytes
SK-Mel-103
c
NT
Bortezomib
shRNA
No Infection control
Mcl-1
Bcl-2 (1)
Bcl-2 (2)
Bcl-xL
Mcl-1
Bcl-2
Bcl-xL
Actin
Melanocytes
SK-Mel-103

Differential impact of Mcl-1, Bcl-x_L and Bcl-2 to the resistance of melanoma cells to bortezomib

Long-term downregulation of either Bcl-2 or Bcl-x_L can induce cell death in melanocytes (120, 121). However, temporal inactivation of these genes by shRNAs (mimicking the acute treatments typical of clinical trials) was well tolerated by both melanoma cells and normal melanocytes (Figure 2.4b). Mcl-1 shRNA was also non-toxic for normal melanocytes. Therefore, isogenic series of normal melanocytes, SK-Mel-19, SK-Mel-103, and SK-Mel-147 (generated by specific inactivation of Mcl-1, Bcl-x_L or Bcl-2), were used as models to address the hierarchical contribution of Bcl-2 family members to bortezomib resistance. The different cell populations were treated with sublethal doses of bortezomib, and cell death was determined by standard trypan blue exclusion at different points after treatment. Partial downregulation of Mcl-1 by antisense RNA has been reported to enhance by two fold the killing activity of bortezomib (97). Our potent shRNA approach showed that further reduction in Mcl-1 levels can have a dramatic impact on the kinetics and final extent of cell death by bortezomib (Figure 2.5a). For example, while more than 50 h were required to kill 70% of the parental SK-Mel-19 (Figure 2.1a), a similar extent of cell death could be achieved by 18 h if Mcl-1 was downregulated (Figure 2.5a). Even for cells such as SK-Mel-103 or -147, with an intrinsically high sensitivity to bortezomib, Mcl-1 downregulation had significant effects (i.e. death rates observed by 18h in Mcl-1 expressing cells, could be achieved as early as 6 h in when Mcl-1 was downregulated; Figure 2.5a). The acceleration of pro-apoptotic events was

assessed by cytochrome *c* (Cyt *c*) release from the mitochondria using standard immunofluorescence (Figure 2.5b). With respect to Bcl-2, its downregulation was surprisingly ineffective in favoring bortezomib-induced cell death, considering the reported potent anti-apoptotic effects of this protein in the response to standard chemotherapeutic agents (122). Thus, neither SK-Mel-19 nor SK-Mel-103 exhibited a change in response to bortezomib when Bcl-2 was downregulated by shRNA (Figure 2.5a,b). Bcl-x_L shRNA however, evinced a noticeable acceleration in the cell killing of both cell lines in response to bortezomib (Figure 2.5a, b; also Figure SX1 for visualization of cell detachment). These results indicate that in addition to Mcl-1, Bcl-x_L should be considered a target of efforts to improve the efficacy of bortezomib.

The roles of Mcl-1, Bcl-x_L and Bcl-2 in cell survival upon proteasome inhibition were also addressed in normal melanocytes. Doses of bortezomib and time points after treatments were similar to those leading to cell death in the melanoma cells. In these conditions, each of these proteins could be highly downregulated (Figure 2.4c) without a significant impact on melanocyte cell viability (Figure 2.5, see also representative micrographs in Figure SX1). Altogether, these results support a differential requirement of Bcl-2 family members for the survival of normal melanocytes and malignant melanoma cells that can provide a therapeutic window for melanoma treatment with proteasome inhibition.

Figure 2.5 Functional impact of inactivation of Bcl-2 family members by RNA interference, and identification of Mcl-1 and Bcl-x_L as primary mediators of the resistance to bortezomib-induced apoptosis. **(a)** Kinetic analysis of cell death measured by trypan blue exclusion after incubation of the indicated isogenic subpopulations of melanocytes or melanoma cells (SK-Mel-19, SK-Mel-103, and SK-Mel-147) with 50 nM bortezomib. **(b)** Release of Cyt *c*. The corresponding isogenic SK-Mel-103 subpopulations expressing scrambled shRNA or shRNA against Mcl-1, Bcl-x_L or Bcl-2 were left untreated or treated with 50 nM bortezomib (Bor) for 6 hours. Cells were fixed and stained with anti-Cyt *c* antibody (green fluorescence). Nuclei were counterstained in blue with DAPI (4',6-diamidino-2-phenylindole). Arrows display cells with cytosolic Cyt *c,* a hallmark of apoptosis, which is most noted in bortezomib-treated cells expressing low levels of Mcl-1.

Figure 2.5

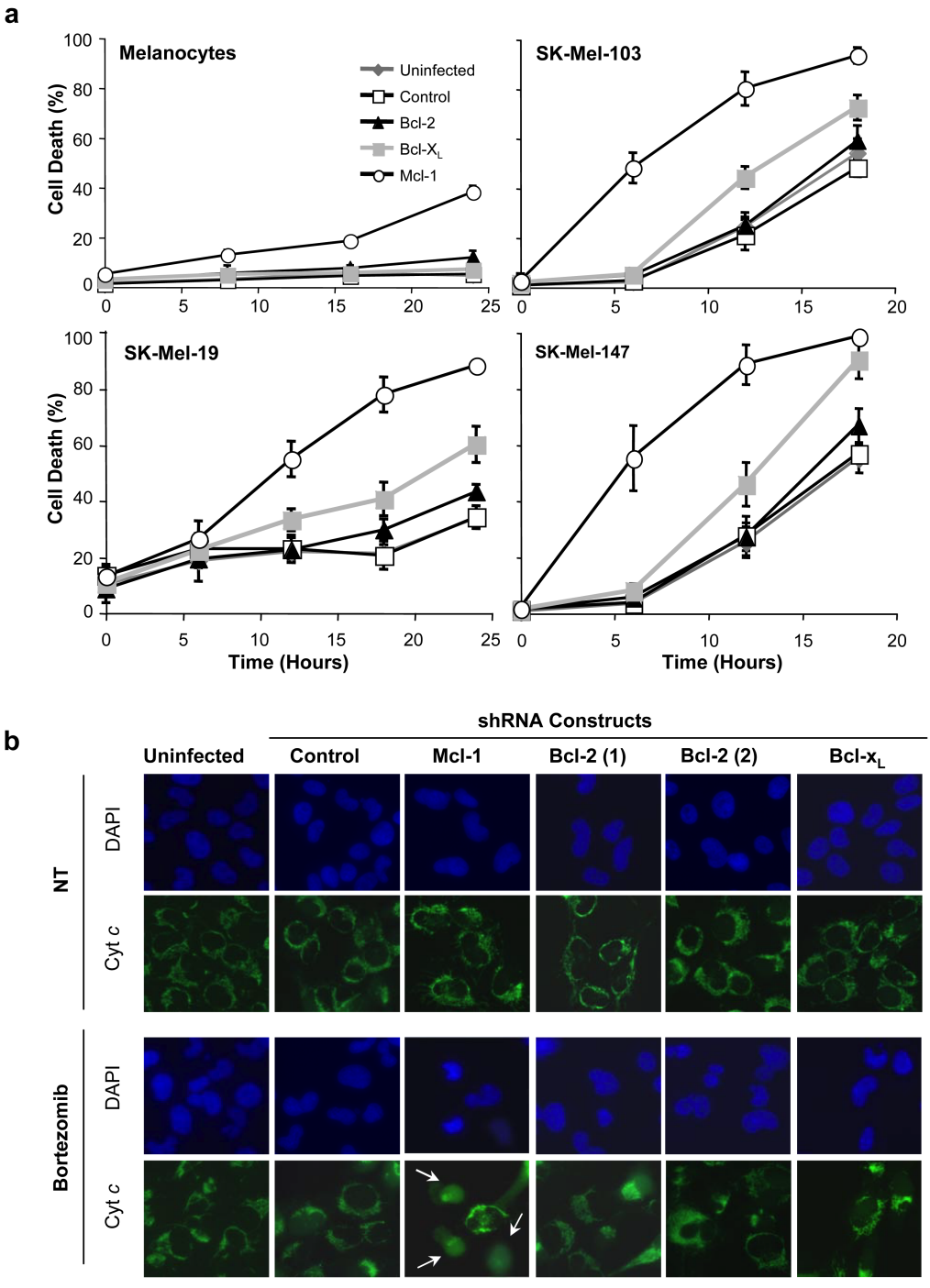
a
Melanocytes
SK-Mel-103
SK-Mel-19
SK-Mel-147
Uninfected
Control
Bcl-2
Bcl-X$_L$
Mcl-1
Cell Death (%)
Time (Hours)
b
shRNA Constructs
Uninfected
Control
Mcl-1
Bcl-2 (1)
Bcl-2 (2)
Bcl-x$_L$
NT
Bortezomib
DAPI
Cyt c

Targeted activation of the apoptotic machinery of aggressive melanoma cells

As indicated above (Figure 2.1), one of the most intriguing features of bortezomib, in melanoma cells and other aggressive cancers, is the lag between the inhibition of the proteasome (typically within 1 h after treatment) and the activation of the apoptotic caspases (24-36 h). Melanoma cells express multiple mechanisms of protection downstream of the release of Cyt *c* and other apoptogenic factors from the mitochondria (23). In this context, whether inhibition of the endogenous levels of Bcl-x_L and Mcl-1 allow for the processing of regulatory and effector caspases, or favor apoptosis independently on caspase activation is unknown. To address this question, SK-Mel-19 and -103 were used as representative examples of cell lines with intrinsically low or intermediate kinetics of caspase processing, respectively (Figure 2.1d,e). Two days after infection with the corresponding shRNA-expressing lentiviruses, cells were treated with low doses of bortezomib, and protein extracts were analyzed by immunoblotting. Consistent with its low impact on cell viability, Bcl-2 shRNA had no impact on caspase cleavage upon bortezomib treatment (Figure 2.6a). However, downregulation of Bcl-x_L, and primarily Mcl-1, showed a marked acceleration of caspase processing (Figure 2.6a). For example, while processing of caspase 9 was barely detectable 24 hours after treatment of the control infected SK-Mel-19 cells, more than 50% of this caspase was cleaved as early as 6 h after treatment when Mcl-1 was downregulated (Figure 2.6a; see quantification in Figure 2.6d). Similarly, compare the minimal cleavage the

effector caspase 3 and caspase 7 in SK-Mel-19 control cells at 18 h of bortezomib treatment, with ≥ 80% processing in the Mcl-1 deficient counterparts (Figure 2.6a and Figure 2.6d). Consistent with feedback loops involving the intrinsic and extrinsic pathways in proteasome-treated cells (49), the processing of caspase 8 was also accelerated by Mcl-1 shRNA interference. Mcl-1 inactivation was also the most potent in promoting caspase processing in the more sensitive SK-Mel-103 (Figure 2.6a).

Mcl-1 can bind to Noxa as well as other partners within the Bcl-2 family. There is an active debate how pro- and anti-apoptotic proteins of this family are inter-regulated to control mitochondrial-dependent death programs (26, 123). To assess the specific contribution of Noxa to bortezomib response following Mcl-1 downregulation, we again exploited RNA interference methods. Specifically, we infected melanoma cells with lentiviruses coding for a highly efficient shRNA against Noxa (56), which is able to completely abrogate even the massive accumulation of this protein that occurs upon proteasome inhibition (see examples in Figure 2.6b). As shown in Figure 2.6c, blockade of Noxa in SK-Mel-19 compromised the effect of Mcl-1 downregulation on bortezomib-mediated cell killing, reducing the level of cell death to below that of parental control cells. These effects were found across a range of bortezomib dosage levels, and across different treatment times, for both SK-Mel-19 and -103 lines (Figure 2.6b, and results not shown). Our results strengthen the model by which inactivation of Mcl-1 is not sufficient *per se* to engage the apoptotic machinery unless there is also an activating signal (which in the case of bortezomib is provided by Noxa).

The shRNA interference used here also provides novel insights on how to efficiently activate the intrinsic apoptotic machinery of melanoma cells, which is otherwise impervious to standard chemotherapeutic agents.

Figure 2.6 shRNA interference to identify genetic alterations allowing for a selective acceleration of caspase processing in melanoma cells. (a) Impact of bortezomib treatment on caspase processing. Protein immunoblots showing the processing of regulatory (casp-9 and casp-8) and effector caspases (casp-3 and casp-7) in melanoma cell lines SK-Mel-19 and SK-Mel-103 expressing the indicated shRNAs. Arrows next to each blot point to the inactive proform of the corresponding caspases, which need to be fully processed for maximal activation of cell death (see Fig. 2.5a). The short dashes mark the cleaved subunits. Note acceleration of caspase processing by bortezomib induced by shRNAs against Mcl-1, and to a lower extent Bcl-x_L, but not Bcl-2 (see quantification in Fig. 2.6d below). **(b)** Generation of NOXA-deficient cells by shRNAs able to downregulate this protein without affecting other Bcl-2 proteins (Mcl-1 is shown here as a reference). Blots corresponds to extracts isolated 3 days after infection of SK-Mel-19 or SK-Mel-103 with NOXA-shRNA expressing lentivirus. **(c)** Response of the indicated cell populations to increasing doses of bortezomib (nM concentration). Data shown represents average ± SE from three experiments, estimated 18h after treatment of SK-Mel-19 and 12h after treatment of SK-Mel-103. **(d)** Caspase processing in representative examples of isogenic series of melanoma cells treated with bortezomib. Graphs correspond to the quantification of protein immunoblots shown in Fig. 2.6a. Processing was estimated with respect to untreated control cells by monitoring the appearance of cleaved forms of regulatory casp-9 and casp-8 and by means of the disappearance of the proform of casp-3 and casp-7. Left graphs correspond to SK-Mel-19 and right graphs to SK-Mel-103.

Figure 2.6

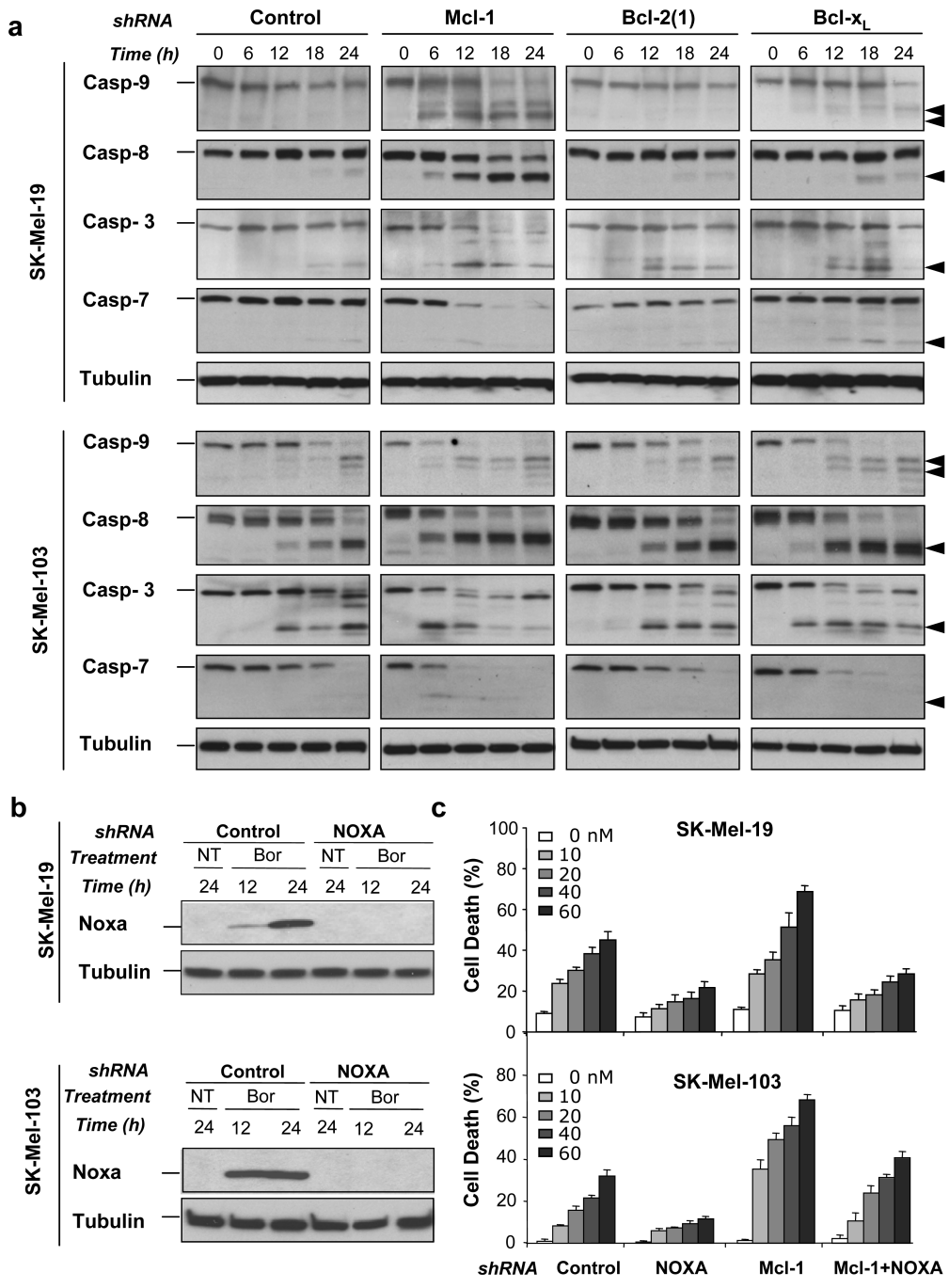
a
shRNA
Control
Mcl-1
Bcl-2(1)
Bcl-x$_L$
Time (h)
0 6 12 18 24
SK-Mel-19
Casp-9
Casp-8
Casp- 3
Casp-7
Tubulin
SK-Mel-103
b
shRNA
Control
NOXA
Treatment
NT
Bor
Time (h)
24 12 24 24 12 24
Noxa
Tubulin
c
SK-Mel-19
SK-Mel-103
Cell Death (%)
0 nM
10
20
40
60
shRNA
Control
NOXA
Mcl-1
Mcl-1+NOXA

Figure 2.6 continued

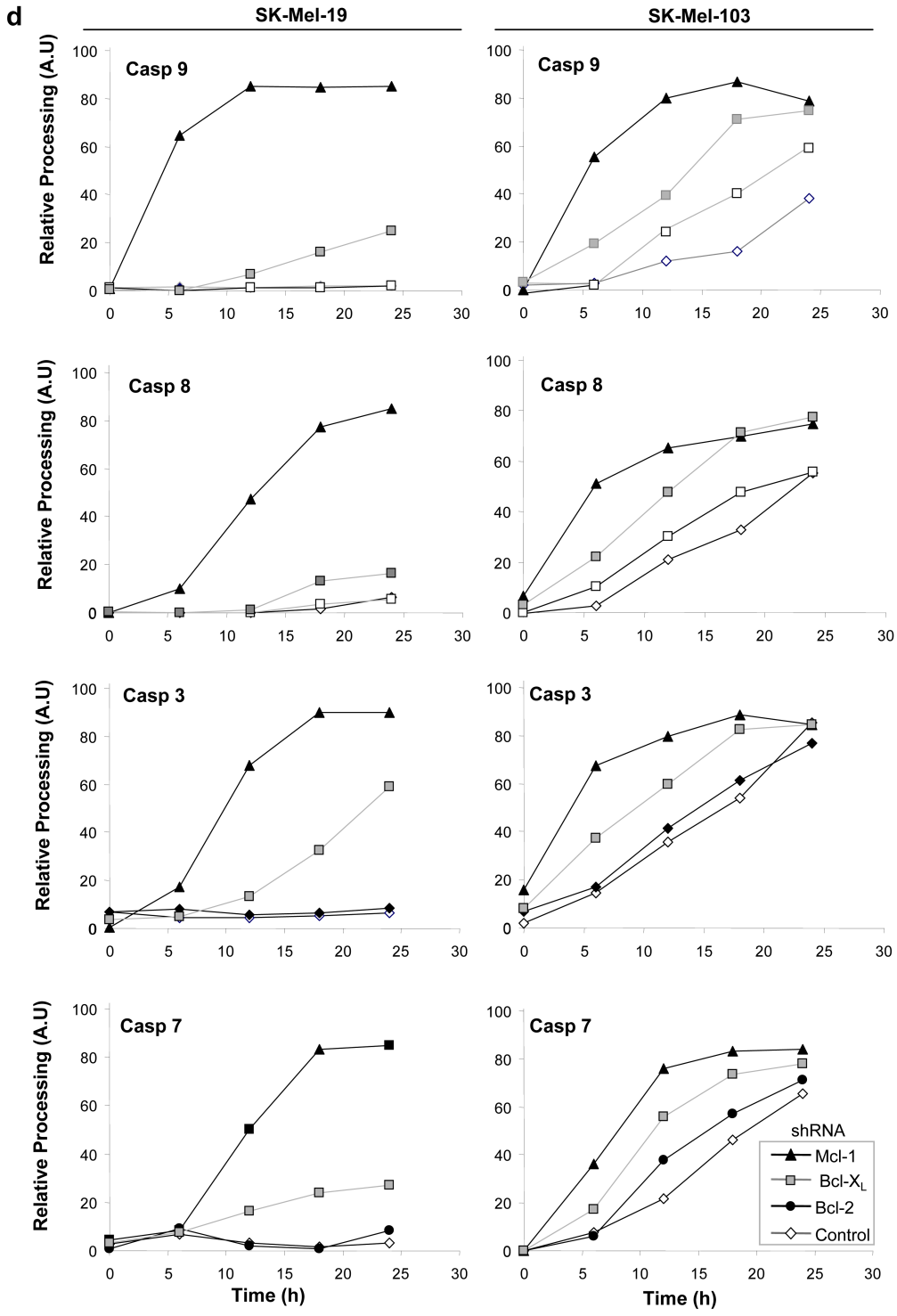

Discussion

In this study, we utilized genetic and pharmacological approaches to identify intrinsic mechanisms of resistance to bortezomib, and provided the proof of principle for a strategy to increase the efficacy of this drug against melanoma *in vivo*. Specifically, we have identified a functional hierarchy in the efficacy of anti-apoptotic Bcl-2 family members in the response to proteasome inhibition that affects the viability of normal melanocytes and melanoma cells in a differential manner. Thus, our highly efficient RNA interference showed a tumor cell specific requirement of Mcl-1 (and to a lesser extent Bcl-x_L) in opposing the pro-apoptotic effects of bortezomib. However, both of these proteins are largely dispensable to maintain the viability of normal melanocytes upon bortezomib treatment, offering a window for therapeutic intervention.

From a translational point of view, compounds able to minimize the delay from proteasomal inhibition to the activation of the apoptotic machinery in a tumor cell-selective manner could have important implications. In culture systems, nearly all tumor cells studied respond to bortezomib (49, 50). However, bortezomib is not a rapid inducer of cell death, and an obstacle to maximal implementation of the anti-neoplastic activity of bortezomib *in vivo* is the fact that its effective concentration and time window for tumor cell recognition and killing may be suboptimal (124). In clinical practice, dose management of bortezomib to limit secondary toxicities results in proteasome inhibition that is neither complete, nor sustained. Bortezomib is typically administered by bolus injection, leaving residual proteasomal activity of 20 to 30% and allowing for recovery between

treatment cycles (124). Moreover, pharmacokinetic and pharmacodynamic analyses indicate rapid inactivation of bortezomib by hepatic detoxification systems (124, 125). Therefore, there is interest in compounds that can synergize with bortezomib without compromising the viability of normal cells. This need is particularly important in melanoma patients, whose average survival at metastatic stages (i.e. 6 to 10 months) could not be improved with the current dosing and administration route of bortezomib.

The rational design of new treatments, which overcome the resistance of melanoma cells to bortezomib, is complicated by several hurdles. First, the ubiquitin/proteasome system controls the half-life of nearly 80% of cellular proteins, both in normal and tumor cells (51), and no consistent predictive markers of response to bortezomib have been identified *in vivo* (50). Furthermore, potent pro-apoptotic factors such as Bim can be induced by proteasome inhibition in melanocytes as efficiently as in their tumor counterparts (see Figure 2.7). Therefore, normal cell compartments may be inherently at risk of stress driven by proteasome inhibition, and thus, rely on potent mechanisms of protection to maintain their viability.

Figure 2.7

Figure 2.7 Differential regulation and requirement of Bcl-2 family members in melanoma cells and melanocytes treated with bortezomib. Bcl-2 family members can be grouped in three categories depending on their regulation by the proteasome: (i) Proteasome independent (e.g. Bcl-2, Bcl-x_L, BAX, BAK; here depicted in black), (ii) regulated by the proteasome in a tumor cell-specific manner (NOXA; shown in red) and (iii) controlled by the proteasome in normal and tumor cells (e.g. Mcl-1 and Bim; shown in blue). Surprisingly, despite the significant induction of Bim in melanocytes, these cells are largely independent of Mcl-1, Bcl-x_L or Bcl-2 for survival. Melanoma cells, however, die in significant numbers if Mcl-1 is blocked. A noticeable acceleration of cell death is also found by blocking Bcl-x_L. Bcl-2, however, was dispensable for the viability of bortezomib-treatment melanoma cells. These results emphasize the non-equivalent functional requirement of Bcl-2 family members in normal melanocytes and melanoma cells that can be exploited for rational drug design.

An additional barrier to drug development for melanoma treatment (as well as for other aggressive solid tumor types) is the typically complex genetic background, with defects in all known cell death pathways, which block the apoptotic machinery upstream and downstream of the mitochondria. In particular, Bcl-2, Bcl-x_L and Mcl-1 can play key roles in controlling both caspase-dependent and independent pathways in response to a variety of chemotherapeutic agents. The functional hierarchy of these anti-apoptotic factors, and their ultimate mechanism of action in the control of melanoma cell maintenance, is unclear. In fact, the interplay between pro- and anti-apoptotic members of this family is under debate in multiple systems (26, 126). According to the so-called "displacement model", Mcl-1, Bcl-2 and Bcl-x_L directly inhibit pro-apoptotic Bax and/or Bak. In this case, competitive BH3 mimetics, or strategies to efficiently block Mcl-1/Bcl-2/Bcl-x_L function, are sufficient to engage mitochondrial dysfunction (30, 105). The "direct binding model" argues that displacement of anti-apoptotic proteins is insufficient to promote cell death and that additional pro-apoptotic inducers are required for full activation of BAX and BAK (100, 127). Our shRNA approach is consistent with this second scenario. Thus, melanoma cells can tolerate an acute downregulation of Mcl-1. Bortezomib can provide the additional signals needed by a potent and tumor cell selective induction of Noxa (see model in Figure 2.7).

Since Noxa preferentially binds to and is countered by Mcl-1 (30, 100), it is not surprising that our potent Mcl-1 shRNA dramatically accelerated bortezomib-driven killing of melanoma cells. However, the fact that Mcl-1 is dispensable for

the viability of normal melanocytes was unexpected, considering that Mcl-1 is a primary blocker of Bim, which is highly induced in melanocytes upon bortezomib treatment (Figure 2.7). In this context, it is also intriguing that neither Bcl-2 nor Bcl-x_L downregulation compromise the viability of bortezomib-treated melanocytes. This dispensability of Mcl-1, Bcl-x_L and Bcl-2 in melanocytes would have been missed in the absence of the potent and selective short hairpin interfering RNAs used in this study.

Our data showing a hierarchical organization of apoptotic modulators in the response of melanoma cells to bortezomib (i.e. Mcl-1>Bcl-x_L>>Bcl-2) have implications for future drug design. Inactivation of Bcl-2 or Bcl-x_L alone may not be sufficient to counteract resistance to proteasome inhibitors. In this context, our results provide a molecular explanation for the only modest enhancement of bortezomib-induced cell death with the BH3 mimetics ABT-737 (109) and BH3I-2' (104), which bind poorly to Mcl-1. Conversely, (-)-gossypol and other BH3 mimetics with high affinity for Mcl-1 and Bcl-x_L could dismantle the shield of protective responses that halt caspase activation in melanoma cells. The significant activity of the (-)-gossypol/bortezomib combination in blocking melanoma cell growth in surrogate models of metastatic dissemination is encouraging considering that these cells are invariably resistant to standard anti-cancer agents. Second-generation BH3 mimetics based on the structure of gossypol are being designed and produced with the objective of improving binding to Mcl-1 (110). These new reagents may ultimately provide a long-term response in combination with bortezomib.

In summary, this study has addressed the interplay between the proteasome and modulators of the apoptotic machinery in melanoma. Our results identify Bcl-2 family members with differential regulation by the proteasome, and of differing importance to the survival of melanocytes *versus* melanoma cells. We provide evidence, both *in vitro* and *in vivo,* for the design of rational combination strategies utilizing BH3 mimetics with high affinity for Mcl-1 to improve the efficacy of proteasome inhibition and overcome chemoresistance in malignant melanoma.

Materials and Methods

Cells

The metastatic melanoma cell lines SK-Mel-19, SK-Mel-29, SK-Mel-103, and SK-Mel-147 were obtained from the Memorial Sloan-Kettering Cancer Center, New York. These cells were cultured in Dulbecco's modified Eagles's medium (DMEM) (Life Technologies, Rockville, MD) supplemented with 10% fetal bovine serum (Nova-Tech, Inc., Grand Island, NY). Human melanocytes were isolated from human neonatal foreskins as described (56) and maintained in Medium 254 supplemented with melanocyte growth factors (HMG-1) containing 10 ng/ml phorbol 12-myristate 13-acetate (Cascade Biologics, Portland, OR).

Reagents

Bortezomib (Velcade™; formerly PS-341) was obtained from Millennium Pharmaceuticals (Cambridge, MA). For analyses in tissue culture systems, bortezomib was reconstituted in DMSO at a concentration of 0.1 mM, and for studies *in vivo* it was prepared in a 0.85% sterile saline solution at a concentration of 1.2 mg/ml. (-)-Gossypol was synthesized as described previously (128). For oral dosing, lyophilized (-)-gossypol was resuspended in 100% ethanol, and subsequently diluted in sterile water to 10% ethanol, for a working concentration of 1.5 mg/ml.

Fluorescence polarization assays

Inhibitory binding constants of (-)-gossypol to purified Bcl-2, Bcl-x_L and Mcl-1 were determined by competitive fluorescence-polarization-based binding assays as described (119). In short, a Bid BH3-containing peptide (residues 79-99) was labeled at the N-terminus with 6-carboxyfluorescein succinimidyl ester (FAM). 1-2.5 nM FAM-Bid peptide were preincubated with purified Bcl-2 (40 nM) or Mcl-1 (5nM) in 100 mM potassium phosphate pH 7.5; 100 μg/ml bovine gamma globulin; 0.02% sodium azide). To determine the Ki values for Bcl-x_L, fluorescence polarization assays were performed with 30 nM Bcl-x_L in 50mM Tris-Bis, pH 7.4 and 0.01% bovine gamma globulin. Polarization values were measured using a Ultra plate reader (Tecan U.S. Inc., Research Triangle Park, NC) in the absence or in the presence of increasing concentrations of (-)-gossypol. Excitation and emission wavelengths were set at 485 nm and 530 nm, respectively. Purified protein or fluorescent probes were also included as reference controls. *K*i values were calculated with GraphPad Prizm 4 software (GraphPad Software, San Diego, CA) using previously described equations (http://sw16.im.med.umich.edu/software/calc_ki/) (111).

Protein immunoblotting

To determine changes in protein levels, 2×10^6 cells were treated with bortezomib (50 nM) and harvested at the indicated time points after treatment. Total cell lysates were subjected to electrophoresis in 12, 15 or 4-15% gradient SDS gels under reducing conditions, and subsequently transferred to Immobilon-P

membranes (Millipore, Bedford, MA). Protein bands were detected by the ECL system (GE Healthcare, Buckinghamshire, UK). Primary antibodies included: caspase-9 and caspase-3 from Novus Biologicals (Littleton, CO); caspase-8 (Ab-3) from Oncogene Research Products (San Diego, CA); caspase-7 from Cell Signaling Technology (Beverly, MA); Bcl-x_L from BD Transduction Laboratories (Franklin Lakes, NJ); Bcl-2 from Dako Diagnostics (Glostrup, Denmark); Noxa from Calbiochem (San Diego, CA); and tubulin (clone AC-74) from Sigma Chemical (St Louis, MO). Secondary antibodies were either anti-mouse or anti-rabbit from GE Healthcare. Image J was used to quantify changes in protein levels induced by bortezomib, considering untreated controls as reference for basal expression. Caspase processing was analyzed by immunoblotting with specific antibodies. Changes in the inactive / cleaved forms of specific caspases were quantified using Image J software and plotted as a function of time.

Cell death assays/Cyt c visualization

The percentage of cell death at the indicated times and drug concentrations was estimated by standard trypan blue exclusion assays. Briefly, floating and adherent cells were pooled, stained with a 0.4% trypan blue solution (Gibco Laboratories, Grand Island, NY) and scored under a light microscope (a minimum of 500 cells per treatment were counted). Cyt *c* localization was visualized by immunofluorescence in cells fixed with 4% formaldehyde essentially as previously described (119). Where indicated, nuclei were stained with DAPI using standard methods.